Dalton Transactions

Accepted Manuscript

ROYAL SOCIETY OF CHEMISTRY

www.rsc.org/dalton

Journal Name

ARTICLE

Synthesis and characterization of ML and ML_2 metal complexes with amino acid substituted bis(2-picolyl)amine ligands

Received 00th January 20xx,
Accepted 00th January 20xx

DOI: 10.1039/x0xx00000x

www.rsc.org/

Đani Škalamera,[a] Ernest Sanders,[a] Robert Vianello,[a] Aleksandra Maršavelski,[a] Andrej Pevec,[b] Iztok Turel[b] and Srećko I. Kirin*[,a]

Metal complexes with **ML** or ML_2 stoichiometry have been isolated in the reaction of $Zn(NO_3)_2$, $ZnBr_2$ or $M(NO_3)_2$ / $Na(BF_4)_2$, M = Zn(II), Co(II) or Ni(II), with either amino acid or amine substituted tridentate nitrogen ligands based on bis(2-picolyl)amine (**bpa**) or bis(2-quinaldyl)amine (**bqa**). The stoichiometry (**M** : **L** = 1:1 or 1:2) and stereochemistry (*mer*, *trans-fac* or *cis-fac*) of the products have been studied by NMR and IR spectroscopy, X-ray single crystal analysis and quantum-chemical calculations with an implicit SMD solvation model.

Introduction

Polypyridyl ligands and their transition metal complexes attract considerable interest in biological and material sciences.[1,2] Among polypyridyl ligands, tridentate ligands **L** with two identical terminal coordination sites like terpyridine (**L** = **terpy**) and bis(2-picolyl) amine (**L** = **bpa**) are investigated as building blocks in a number of areas, including chemosensors, catalysts and biomedicinal applications.[3]

Transition metal complexes of tridentate ligands **L** are well known for both **ML** and ML_2 stoichiometries. In **ML** complexes, the tridentate ligand **L** can be bound to the central metal atom in meridional (*mer*) or facial (*fac*) fashion,[4-6] **Fig. 1**; the remaining coordination sites are usually occupied by counter-ions and / or solvent molecules. The ML_2 complexes can adopt several six-coordinated geometrical isomers: meridional (*mer*), *trans*-facial (*trans-fac*), and Δ or Λ *cis*-facial (*cis-fac*), **Fig. 1**. For the rigid **terpy** ligand, the meridional isomers of the corresponding **M(terpy)** or $M(terpy)_2$ metal complexes are strongly preferred, while complexes with the more flexible ligands like **bpa** can form both meridional and facial isomers. Factors governing the stoichiometry and stereochemistry of those complexes are currently not well understood.

Continuing our interest in transition metal complexes of nitrogen ligand amino acid bioconjugates,[4d,7] we present herein the preparative, spectroscopic, crystallographic and computational study of complexes with amino acid or amine substituted bis(2-picolyl)amine ligands and late transition metals, M = Zn(II), Ni(II) or Co(II). Particular emphasis has been placed on several synthetic protocols using different anions and solvents as well as properties of the resulting metal complexes, including their stoichiometry and stereochemistry.

Results and discussion

Ligands

Bis(2-picolyl)amine ligands **L1** - **L5** were synthesized in good yields by nucleophilic substitution in acetonitrile (ACN) using two equivalents of 2-picolyl (or 2-quinaldyl) chloride hydrochloride and one equivalent of an *N*-deprotected amino acid or primary amine, **Scheme 1**, and characterized by ^{1}H, ^{13}C NMR spectroscopy and ESI mass spectrometry.

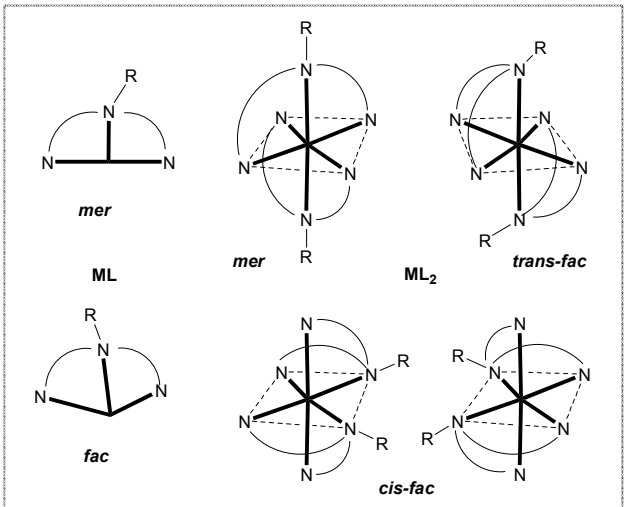

Fig. 1. Schematic representation of geometrical isomers of **ML** and ML_2 metal complexes. The central metal atom **M** and other substituents on **ML** complexes (counter-ions, solvent molecules) are omitted for clarity.

[a] Ruđer Bošković Institute, Bijenička cesta 54, 10 000 Zagreb, Croatia. E-mail: Srecko.Kirin@irb.hr
[b] Faculty of Chemistry and Chemical Technology, University of Ljubljana, Večna pot 113, 1000 Ljubljana, Slovenia

Electronic Supplementary Information (ESI) available: Spectroscopic characterization of ligands and complexes (^{1}H, ^{13}C NMR, ESI MS), Cartesian coordinates for all computed molecules in a single separate text file, crystallographic data in cif format. CCDC 1418408–1418417. For ESI see DOI: 10.1039/x0xx00000x

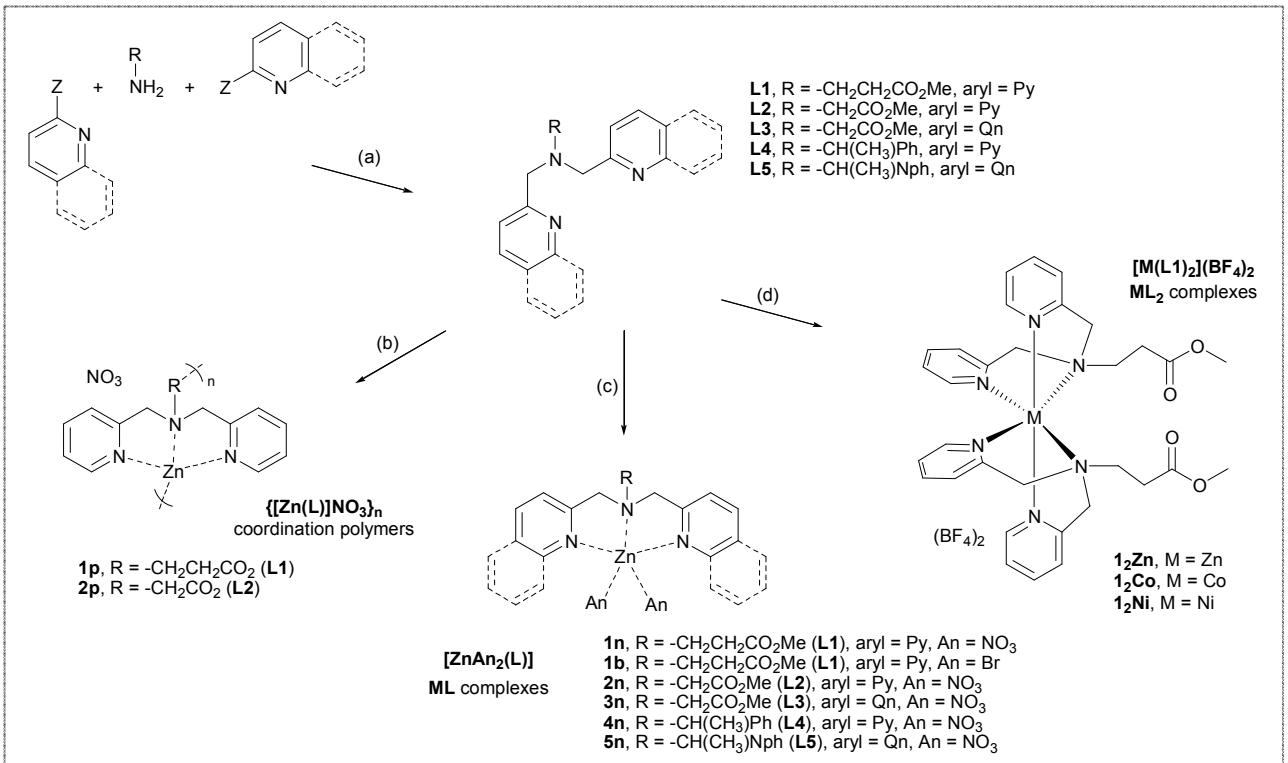

Scheme 1. Synthesis of ligands **L1** – **L5** and metal complexes: Coordination polymers (**1p**, **2p**), **ML** complexes (**1b**, **1n**-**5n**) and **ML$_2$** complexes **1$_2$M**, M = Zn, Co or Ni. In **1p** and **2p**, the methyl ester group of the corresponding ligand **L1** or **L2** is hydrolyzed. Reaction conditions: (a) K_2CO_3, KI, CH_3CN, 3d; (b) $Zn(NO_3)_2$, CH_3OH; (c) $ZnAn_2$, CH_3OH (or CH_3CN); (d) 1. $M(NO_3)_2$, CH_3OH, 2. $Na(BF_4)_2$, CH_3OH; Z = -CH_2Cl, An = NO_3 or Br, M = Zn(II), Co(II) or Ni(II).

Metal complexes, synthesis and crystallography

First attempts to prepare metal complexes with **ML$_2$** stoichiometry were performed using Zn nitrate and ligands **L1** or **L2**, respectively, **Scheme 1**. Slow evaporation of the reaction mixtures to dryness yielded a small amount of crystalline products **1p** or **2p**, respectively. X-ray single crystal analysis revealed that both **1p** and **2p** are coordination polymers with 1:1 ligand to metal stoichiometry, despite the 1:2 ratio used in the synthesis (**M** : 2 **L**). In addition, cleavage of the ester group occurred in both cases that could be rationalized by the rather prolonged reaction time.[8] ORTEP diagrams of **1p** and **2p** are shown in **Fig. 2**, while selected bond lengths and angles are highlighted in **Table 1**. Experimental data for all X–ray diffraction studies in this publication are collected in **Tables 3** and **4**.

Coordination polymer **1p**, with the composition {[**Zn(L1)]NO$_3$ × Et$_2$O)}$_n$**, features an N_3O_3 distorted octahedral coordination polyhedron, including a meridionally bound **bpa** ligand, with 16.5° angle between the pyridine ring planes, as well as one intra- and two intermolecular coordinated carboxylic oxygen atoms. In **1p**, the **bpa** acts as a tetradentate ligand to one metal atom and a

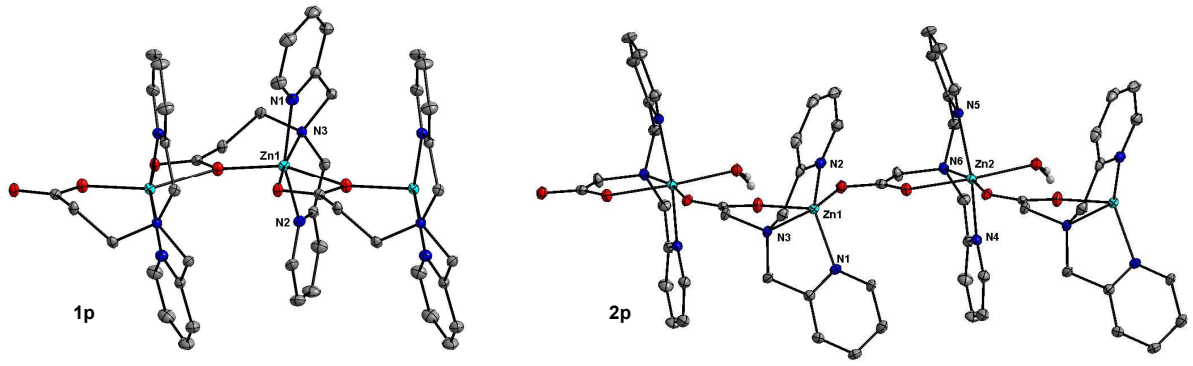

Fig. 2. Molecular structure of coordination polymers **1p** (left) and **2p** (right). Displacement ellipsoids were drawn at the 30% probability level. The hydrogen atoms bonded to carbon, NO_3^- anions, solvent molecules (Et_2O for **1p** and CH_3CN for **2p**) and non-coordinated water molecules (for **2p**) were omitted for clarity.

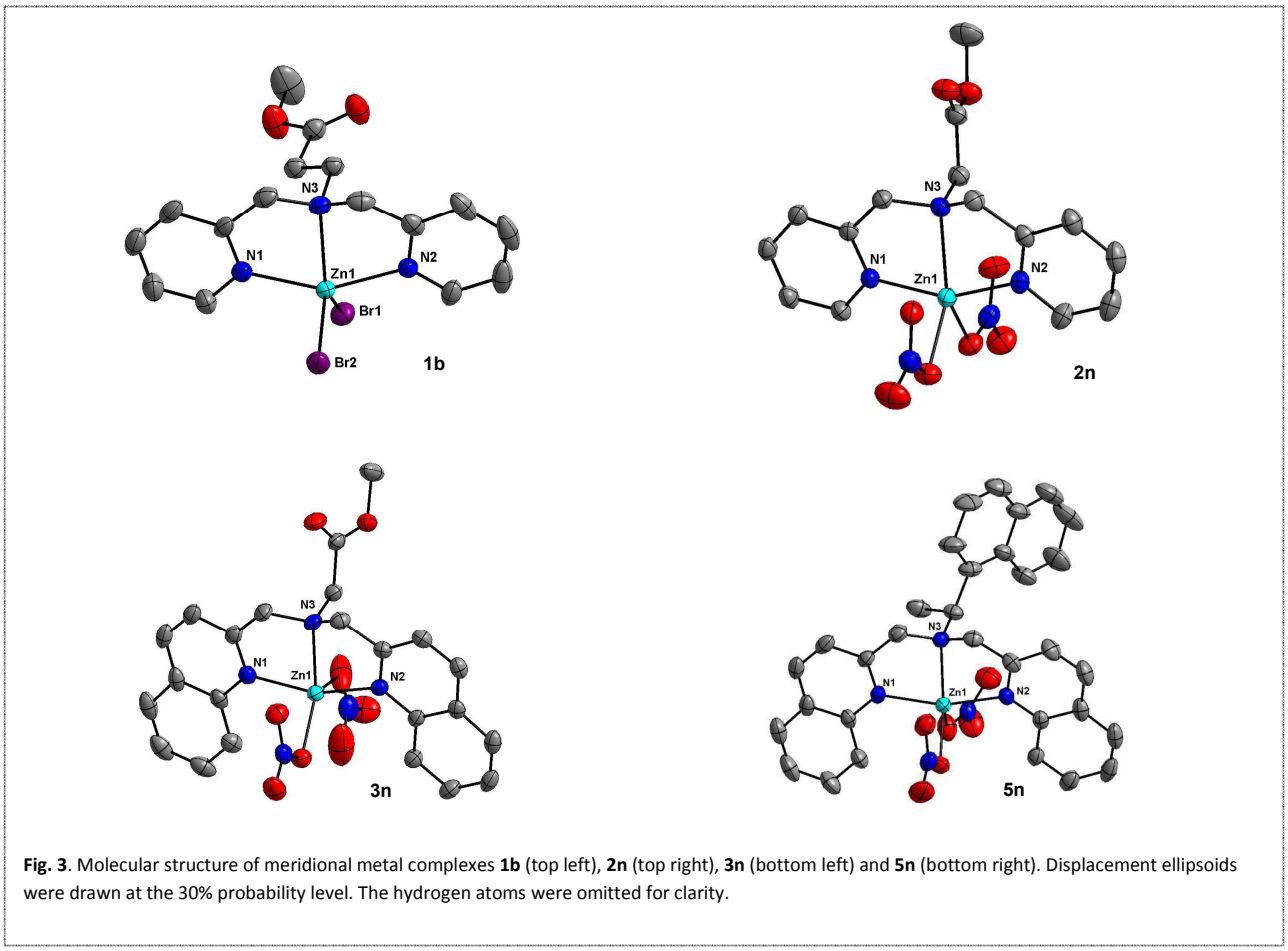

Fig. 3. Molecular structure of meridional metal complexes **1b** (top left), **2n** (top right), **3n** (bottom left) and **5n** (bottom right). Displacement ellipsoids were drawn at the 30% probability level. The hydrogen atoms were omitted for clarity.

bidentate ligand to the neighbouring metal atom. The second coordination polymer **2p** has the composition **{[Zn(bpaCH$_2$CO$_2$)] [Zn(bpaCH$_2$CO$_2$)(H$_2$O)]}$_n$ (NO$_3$)$_{2n}$ × (H$_2$O)$_n$ × (CH$_3$CN)$_n$** and contains alternating monomer building blocks with different coordination geometries. One monomer building block in **2p** reveals an N_3O_2 distorted trigonal bipyramidal coordination (τ = 0.68),[9] while the other monomer contains an N_3O_3 distorted octahedral coordination. Detailed representation of both coordination geometries in **2p** is shown in **Fig. 42** (see ESI). The major difference between the two coordination geometries is an additionally bound solvent water molecule in the later monomer of **2p**. In both monomer units of **2p**, the meridionally bound ligand is tetradentate to one metal atom and monodentate to the neighbouring one.

Intermolecular side chain coordination results in the formation of *zig-zag* polymeric chains along the crystallographic *b* axis in **1p** and along the *a* axis in **2p**, respectively. In addition, intra-molecular side chain coordination in **1p** and **2p** forms favorable six-membered or five-membered chelate rings, respectively. In the literature, similar transition metal *zig-zag* coordination polymers are described with general formula **[M{bpa-(CH$_2$)$_m$-CO$_2$)}]$_n$(anion)$_n$**, M = Zn(II), Cu(II), Co(II) or Mn(II), m = 1 or 2.[4d,10] However, if the **bpa** ligand is substituted with a longer aliphatic chain, m ≥ 3, intra-molecular coordination of carboxylic oxygen atoms to the metal would cause a less favorable seven-membered or larger chelate ring. Therefore, in such cases both carboxyl oxygen atoms coordinate to the neighboring molecule in the polymeric chain.[10a,b]

A possible reason for the formation of an 1:1 complex in both **1p** and **2p** could be the hydrolysis of the ester group and consequently the **bpa** acting as tetra- or pentadentate ligand, preventing the attachment of a second ligand. Attempts to suppress ester hydrolysis included (a) shorter reaction times in the preparation of **1n** and **2n**, (b) changing the anion from nitrate to bromide in **1b** and (c) changing the **bpa** ligand with a larger, slower reacting bis(2-quinaldyl)amine (**bqa**) ligand in **3n** and **5n**. In addition, phenylethylamine (Pea) or naphthethylamine (Nea) substituted ligands without an ester group were used in **4n** or **5n**, respectively. However, in all cases only **ML** complexes precipitate from the reaction mixture (methanol or acetonitrile solution), even if a 1:2 metal to ligand stoichiometry was applied in the preparation, see experimental section. Single crystals of **1b**, **4n** and **5n**, were successfully grown by slow evaporation of a methanol solution, while diffusion of diethyl ether in a methanol solution of the corresponding complex was used for **2n** and **3n**. The ORTEP plots of the crystal structures are shown in **Fig. 3 and 4**, while selected bond lengths and angles are highlighted in **Table 1**.

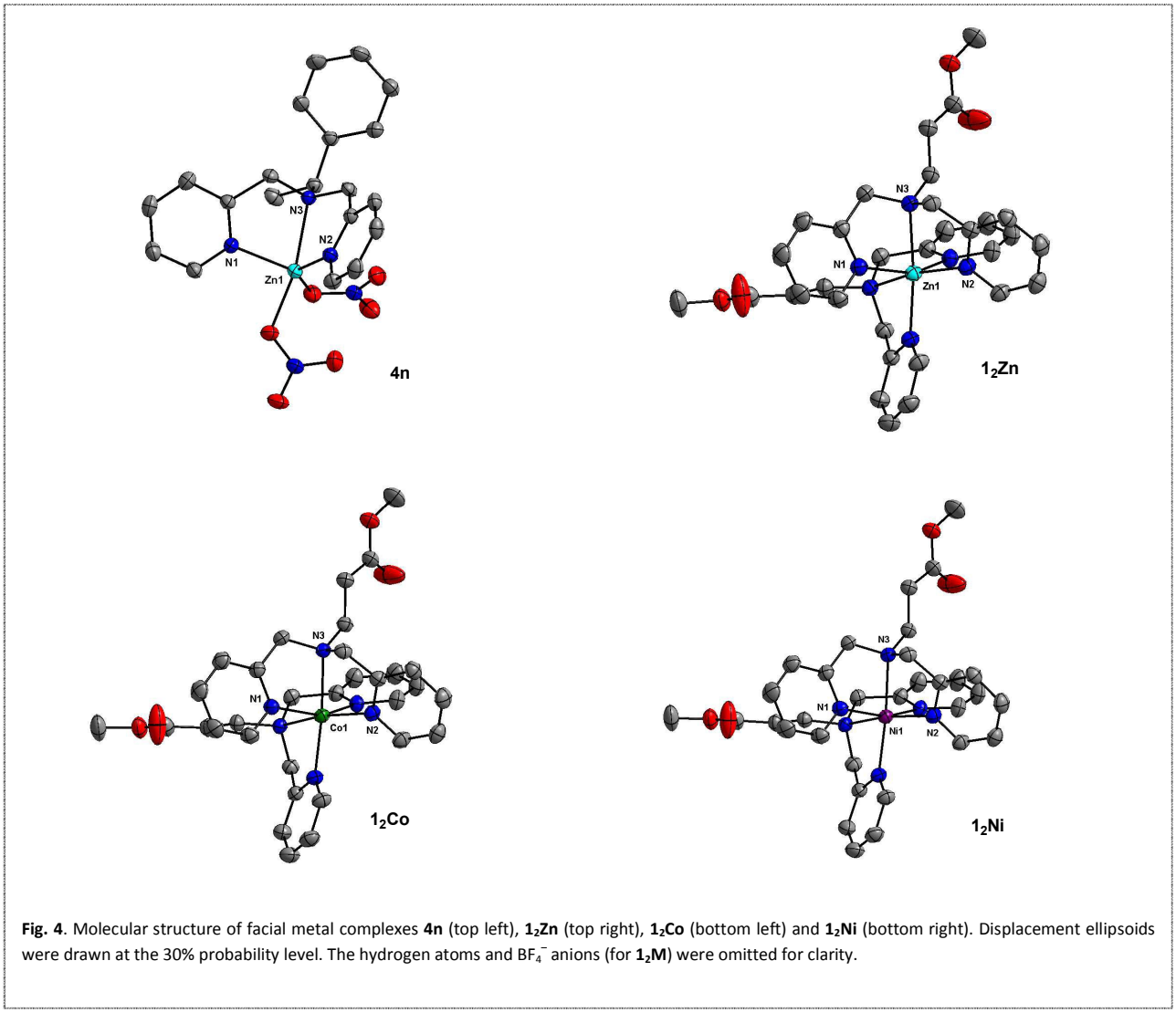

Fig. 4. Molecular structure of facial metal complexes **4n** (top left), **1_2Zn** (top right), **1_2Co** (bottom left) and **1_2Ni** (bottom right). Displacement ellipsoids were drawn at the 30% probability level. The hydrogen atoms and BF_4^- anions (for **1_2M**) were omitted for clarity.

Compounds **[$ZnBr_2$(L1)] 1b**, **[$Zn(NO_3)_2$(L2)] 2n**, **[$Zn(NO_3)_2$(L3)] 3n**, **[$Zn(NO_3)_2$(L4)] 4n** and **[$Zn(NO_3)_2$(L5)] 5n** are mononuclear complexes with **ML** stoichiometry. They feature the **bpa** or **bqa** as tridentate ligand with two counter-ions (bromide or nitrate) coordinated to the central metal atom, resulting in a distorted trigonal bipyramidal geometry N_3Br_2 or N_3O_2, respectively. The tau parameter was calculated for these complexes to measure the grade of distortion: τ = 0.47 (**1b**), 0.24 (**2n**), 0.30 (**3n**), 0.59 (**4n**) and 0.30 (**5n**).[9] These τ values demonstrate that in these complexes the geometry around the zinc atom is extremely distorted trigonal bipyramidal, suggesting a distortion towards the square-based pyramidal arrangement. It is interesting to note that the ligand is coordinated meridionally in **1b**, **2n**, **3n** and **5n**, with a 10.5°, 4.1°, 4.9° and 5.9° angle between the two heteroaromatic ring planes, respectively. On the other hand, in complex **4n** the **bpa** ligand adopts a facial coordination, with a 67.5° py - py angle. A significantly higher prevalence for the meridional coordination in **[$Zn(An)_2$(bpa)]** complexes is also confirmed by our computations (see later).

Obviously, the **bpa** or **bqa** ligands with a free carboxylic acid functional group are not the only reason for obtaining complexes with 1:1 instead of an 1:2 metal to ligand ratio. Therefore, the anion was exchanged with the non-coordinating tetrafluoroborate, in order to test if the type of anion affects the stoichiometry of the resulting metal complex. In particular, ligand **L1** was first reacted with $Zn(NO_3)_2$ and then with an excess of $NaBF_4$. Complex **1_2Zn** was obtained by diffusion of diethyl ether to the reaction mixture. X-ray single crystal analysis of **1_2Zn** revealed a discrete mononuclear complex **[$Zn(L1)_2$](BF_4)$_2$** with *cis-fac* geometry. The same procedure was successful for obtaining isomorphus complexes **1_2Co** and **1_2Ni** using $Co(NO_3)_2$ or $Ni(NO_3)_2$, respectively. ORTEP plots for **1_2Zn**, **1_2Co** and **1_2Ni** are shown in **Fig. 4**, selected bond lengths and angles are listed in **Table 1**. IR spectroscopy revealed almost identical spectra for **1_2Zn**, **1_2Co** and **1_2Ni**, further supporting isomorphism in the solid state. Attempts to prepare the **[$Cu(L1)_2$](BF_4)$_2$** complex by the same procedure ($Cu(NO_3)_2$, followed by $NaBF_4$) were not successful, presumably the binding of two **bpa** ligands is difficult in a Jahn-Teller distorted octahedral geometry preferred for Cu(II).

Table 1. Selected bond lengths (Å) and angles (º) for metal complexes with structures determined experimentally or by computations.

	1p [a]	**2p** [a,b]	**1b** [a]	**2n** [a]	**3n** [a]	***mer*-[ZnBr$_2$(Me-bpa)]** [c]
M-N1	2.0913(18)	2.057(4) 2.136(4)	2.139(5)	2.068(3)	2.139(4)	2.216
M-N2	2.0815(17)	2.062(4) 2.130(4)	2.179(5)	2.059(4)	2.153(3)	2.218
M-N3	2.1736(16)	2.219(4) 2.217(4)	2.233(4)	2.306(3)	2.179(3)	2.219
N1-M1-N2	154.53(7)	123.11(16) 156.33(16)	151.98(18)	154.61(15)	157.17(14)	148.5
N1-M1-N3	78.80(6)	80.58(15) 77.87(15)	76.30(18)	77.19(13)	79.83(13)	75.0
N2-M1-N3	80.73(6)	79.87(15) 78.58(15)	75.68(17)	77.53(13)	78.50(13)	75.1

	4n [a]	**5n** [a]	**1$_2$Zn** [a]	**1$_2$Co** [a]	**1$_2$Ni** [a]	***cis-fac*-[Zn(Me-bpa)$_2$]$^{2+}$** [c]
M-N1	2.083(4)	2.114(4)	2.2131(15)	2.172(2)	2.1431(14)	2.198 2.199
M-N2	2.040(4)	2.126(4)	2.1072(14)	2.104(2)	2.0704(14)	2.265 2.263
M-N3	2.295(3)	2.198(4)	2.2969(15)	2.280(2)	2.2248(14)	2.264
N1-M1-N2	111.33(15)	158.21(19)	105.62(6)	105.21(9)	102.73(6)	105.2
N1-M1-N3	79.04(14)	80.15(19)	73.75(5)	74.46(8)	75.78(5)	79.0
N2-M1-N3	78.72(14)	79.84(17)	78.60(5)	78.16(8)	79.73(5)	78.3

[a] determined by X-ray single crystal analysis; [b] for **2p**: N1, N2, N3 (penta-coordinated monomer) and N4, N5, N6 (hexa-coordinated monomer); [c] calculated using the (SMD)/M05-2X/6-31+G(d) model.

NMR spectroscopic study

NMR spectroscopy can be used in order to distinguish between the free **bpa** ligand, the 1:1 complex **[Zn(bpa)]$^{n+}$** and 1:2 complexes *cis-fac*-**[Zn(bpa)$_2$]$^{n+}$** or *trans-fac*-**[Zn(bpa)$_2$]$^{n+}$**. In particular, the Py$_\alpha$ protons in ^{1}H NMR are magnetically equivalent in the free **bpa** ligand, while their chemical equivalence is lost in the **bpa** metal complexes due to prohibited amine nitrogen inversion caused by metal coordination. As a consequence, in **[Zn(bpa)]$^{n+}$** two doublets with large geminal coupling are found for Py$_\alpha$. In *cis-fac* complex **[Zn(bpa)$_2$]$^{n+}$**, Py$_\alpha$ groups can be assigned as axial and equatorial (Figure 5d, respectively), and reveal four doublets for the Py$_\alpha$ protons.[6a] An NMR spectroscopic study was performed on Zn complexes of the **L1** ligand with different counter-ions, namely NO_3^-, Br^- and BF_4^-.

First, **ML** complexes were studied by ^{1}H NMR, **Fig. 5a**. Complex **1n** with nitrate counter-ion was taken; the ^{1}H NMR of **1n** in acetonitrile-d$_3$ at room temperature shows two doublets with large germinal coupling for Py$_\alpha$ protons, as expected for an **ML** complex. In contrast, the isolated complex **1b** with bromide counter-ion shows only one singlet for Py$_\alpha$ protons in the ^{1}H NMR (CD$_3$CN) at room temperature, but the Py$_\alpha$ protons split in two doublets at lower temperature (-40 °C). This result can be rationalized if a rather weak bond is assumed between the central zinc atom and the amine nitrogen atom of the **bpa** ligand at room temperature that allows nitrogen inversion and results in a magnetic equivalence of the Py$_\alpha$ protons. At -40 °C the Zn - amine bond is stronger, the nitrogen inversion is hindered and the Py$_\alpha$ equivalence is lost.

Second, **ML$_2$** complexes were investigated by ^{1}H NMR spectroscopy, **Fig. 5b**. The isolated complex **1$_2$Zn** with BF_4^- counter-ion reveals broad signals in CD$_3$CN at room temperature, while at -40 °C signals of the **ML$_2$** complex **1$_2$Zn** were present. In particular, the Py$_\alpha$ protons are split in four doublets, due to further non-equivalence of equatorial and axial Py$_\alpha$ protons in *cis-fac* **1$_2$Zn**. Interestingly, a mixture of the **ML** complex and free ligand **L1** was found in DMSO-d$_6$ at room temperature (RT).

Finally, the ^{13}C NMR spectra of **L1**, **1n** and **1$_2$Zn** were measured and compared, **Fig. 5c**. The two 2-pyridylmethly moieties are magnetically equivalent in both the ligand **L1** and in the **ML** complex **1n**. On the contrary, in the *cis-fac* complex **1$_2$Zn** the 2-pyridylmethly groups are no longer equivalent and two sets of signals can be distinguished (equatorial, eq, and axial, ax).[11] In addition, the ^{13}C NMR spectrum of **1$_2$Zn** in DMSO-d$_6$ shows two sets of signals not only for the 2-pyridylmethly moiety but also for the aliphatic chain, further supporting the **M(L1)** + **L1** assignment mentioned above.

Computational study

Computational analysis was performed with the aim to investigate the relative stability of Zn^{2+} complexes in the acetonitrile solution, and to rationalize the observed trends in the binding affinities; **Me-bpa** was employed as a model ligand and bromide as counter-ion, **Fig. 6**. Three conformations were calculated for **[Zn(Me-bpa)$_2$]$^{2+}$** complexes, namely *mer*, *trans-fac* and *cis-fac*, while two conformations were considered for **[Zn(Me-bpa)]$^{2+}$** complexes (*mer* and *fac*). Furthermore, for the latter 1:1 coordination, calculations were performed taking into account additional coordination of up to three bromide counter-ions and three acetonitrile solvent molecules to add to a maximum of six-coordination sites to the central Zn^{2+} ion. Finally, corresponding complexes with closely related ligands **Me-terpy** and **Me-deta** (Me-diethylenetriamine),[12] as well as simple pyridine or aliphatic nitrogen ligands were used

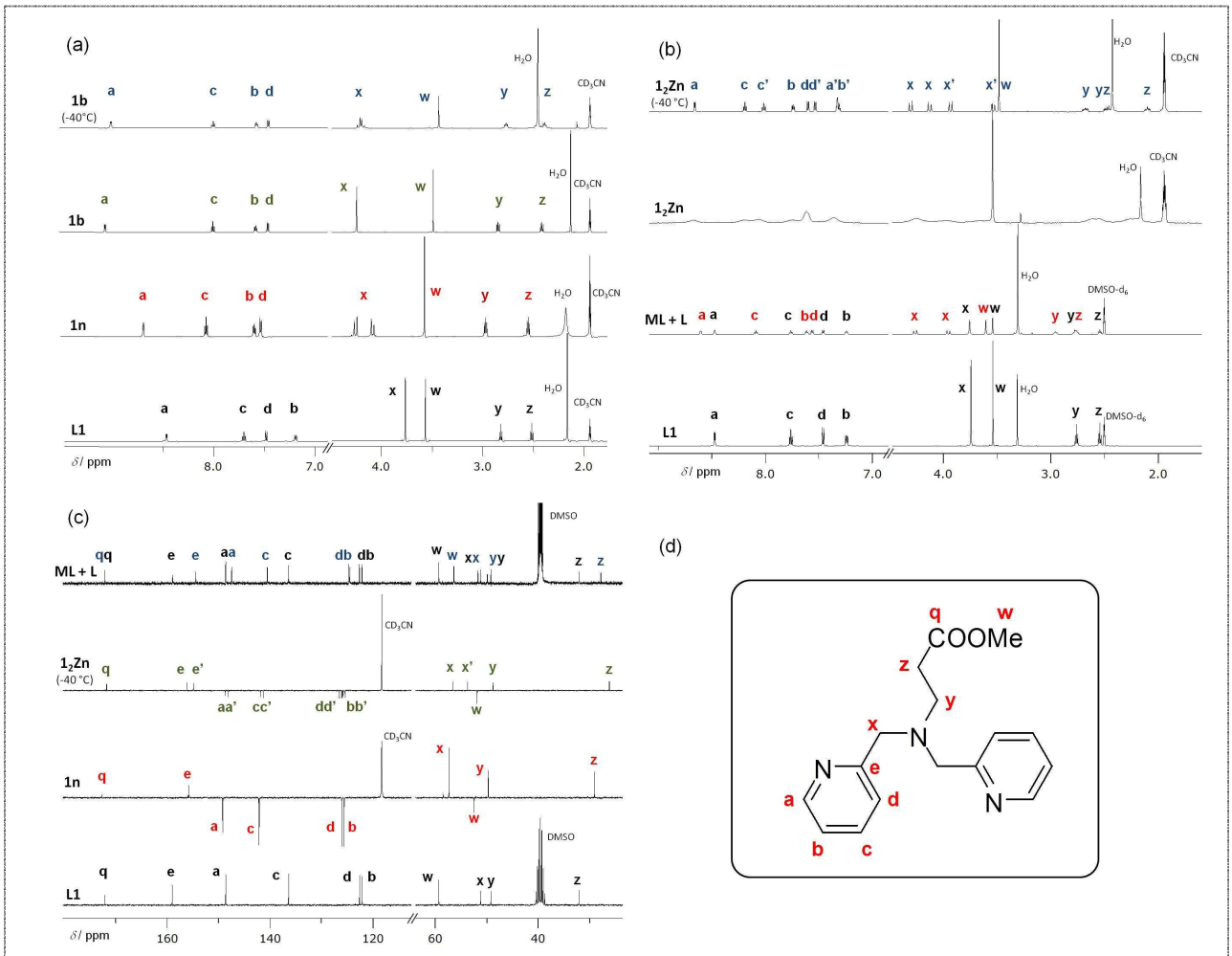

Fig. 5. NMR spectra of ligand **L1** and its Zn complexes **ML** and **ML$_2$** with different counter-ions (Br^-, NO_3^- or BF_4^-): (a) ^{1}H NMR (CD_3CN) spectra, from bottom to top: **L1**, **1n**, **1b** and **1b** (at -40 °C); (b) ^{1}H NMR spectra from bottom to top: **L1** (DMSO-d_6), **1$_2$Zn** (DMSO-d_6), **1$_2$Zn** (CD_3CN) and **1$_2$Zn** (CD_3CN, -40 °C); (c) ^{13}C NMR spectra, from bottom to top: **L1** (DMSO-d_6), **1n** (CD_3CN), **1$_2$Zn** (CD_3CN, at -40 °C), **1$_2$Zn** (DMSO-d_6); (d) numbering scheme of ligand **L1**. If not mentioned otherwise, the spectra are recorded at room temperature.

for comparison, **Fig. 6**. For the calculations a two step procedure was used: molecular dynamics (MD) was applied to identify up to five most stable conformers, that were further optimized by quantum mechanical M05-2X/6-31+G(d) model, with an implicit SMD solvation (see Computational details). All computational results are presented in **Table 2**, and correspond to interaction free energies in acetonitrile, ΔG_{INT}, calculated as the difference between the total free energy of each complex and the corresponding values for its components.

The value calculated for the isolated Zn^{2+} cation, ΔG_{INT} = –465.0 kcal/mol, is in a rather decent agreement with the experimentally determined Zn^{2+} solvation free energies of –454.2 and –477.2 kcal/mol,[13] thus lending credence to the computational setup and results presented herein, which is further prompted by excellent agreement in the selected geometrical parameters (Table 1). Adding the first explicit solvent molecule to the Zn^{2+} coordination gives a stable complex **[Zn(ACN)]$^{2+}$** with ΔG_{INT} = –2.4 kcal/mol and Zn–N distance of 2.123 Å (experimental value is 2.11 Å).[13] However, the second solvent molecules makes this process endergonic, and this trend is continued for up to six solvent molecules in an octahedral arrangement around Zn^{2+}, in a way that every subsequent acetonitrile molecule makes the corresponding ΔG_{INT} value more positive, reaching ΔG_{INT} = 22.6 kcal/mol for

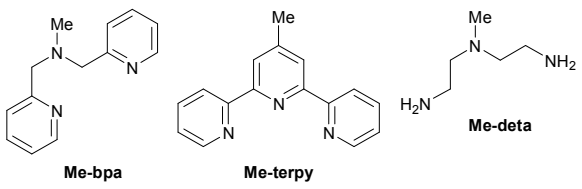

Fig 6. Ligands **Me-bpa**, **Me-terpy** and **Me-deta** used in the calculations, both **[Zn(L)$_2$]$^{2+}$** and **[Zn(L)]$^{2+}$** complexes were investigated.

Table 2. Calculated interaction free-energies ΔG_{INT} in acetonitrile (in kcal mol^{-1}). Experimental pK_a values for ligands are taken from reference 15.

species	ΔG_{INT}	pK_a	species	ΔG_{INT}	species	ΔG_{INT}
Zn^{2+}	–465.0		$[Zn(ACN)]^{2+}$	–2.4	$[ZnBr]^{+}$	–0.8
Br^{-}	–53.6		$[Zn(ACN)_2]^{2+}$	0.8	$[ZnBr_2]$	–4.8
ACN	–6.9		$[Zn(ACN)_3]^{2+}$	5.9	$[ZnBr_2(ACN)]$	–14.4
$[Zn(p\text{-Me-pyridine})]^{2+}$	–11.3	13.3	$[Zn(ACN)_4]^{2+}$	11.3	$[ZnBr_2(ACN)_2]$	–18.7
$[Zn(Py)]^{2+}$	–9.9	12.5	$[Zn(ACN)_5]^{2+}$	16.3	$[ZnBr_2(ACN)_3]$	–9.9
$[Zn(NMe_3)]^{2+}$	–14.0	18.2	$[Zn(ACN)_6]^{2+}$	22.6	$[ZnBr_2(ACN)_4]$	–1.6
$[Zn(NH_2Me)]^{2+}$	–12.2	18.4				
$[Zn(NH_3)]^{2+}$	–11.2	16.5				

ligand	Me-terpy		Me-bpa		Me-deta	
conformation	*mer*	*fac*	*mer*	*fac*	*mer*	*fac*
$[Zn(\mathbf{ligand})]^{2+}$	–25.3	goes to *mer*	–28.8	–25.3	–32.3	–29.9
$[Zn(\mathbf{ligand})(ACN)]^{2+}$	–20.5	goes to *mer*	–22.8	–20.3	–26.5	–23.8
$[Zn(\mathbf{ligand})(ACN)_2]^{2+}$	–15.0	goes to *mer*	–16.9	–13.2	–20.0	–17.9
$[Zn(\mathbf{ligand})(ACN)_3]^{2+}$	–7.5	goes to *mer*	–9.5	–8.4	–11.9	–10.9
$[ZnBr(\mathbf{ligand})]^{+}$	–29.9	goes to *mer*	–36.8	–37.1	–41.3	–38.1
$[ZnBr_2(\mathbf{ligand})]$	–44.4	goes to *mer*	–47.7	–46.1	–49.9	–45.2
$[ZnBr_3(\mathbf{ligand})]^{-}$	–37.7	goes to *mer*	–39.4	–39.4	–45.5	–41.2
$[Zn(\mathbf{ligand})_2]^{2+}$	–39.4	goes to *mer*	–38.3	–36.7 (*cis*) –36.3 (*trans*)	–45.7	–40.2 (*cis*) –41.5 (*trans*)

$[Zn(ACN)_6]^{2+}$. These results strongly suggest that Zn^{2+} cation is solvated with bulk solvation in acetonitrile, and that individual solvent molecules, with the exception of the first one, do not prefer to directly enter in the zinc coordination sphere, which is a noteworthy result. On the other hand, $ZnBr_2$ is rather stable in acetonitrile with ΔG_{INT} = –4.8 kcal/mol and Zn–Br distances of 2.432 Å, implying that it will unlikely spontaneously dissociate to Zn^{2+} and two Br^{-}. Removing one Br^{-} to give **$[ZnBr]^{+}$**, however, makes the dissociation process feasible, being almost in equilibrium with separated Zn^{2+} and one Br^{-} (ΔG_{INT} = –0.8 kcal/mol). Interestingly, adding acetonitrile molecules to the remaining Zn-coordination sites in $ZnBr_2$ increases the stability of **$[ZnBr_2(ACN)_n]$** (n = 0–4) up to n = 2, which assumes tetrahedral geometry with Zn–Br and Zn–N distances of 2.407 and 2.101 Å, respectively, indicating that **$[ZnBr_2(ACN)_2]$** is the predominant species in acetonitrile solution of zinc bromide.[14]

Complexation of Zn^{2+} with the first **Me-bpa** ligand is possible in two conformations and our results indicate that the *mer* isomer is more stable by 3.5 kcal/mol. Its ΔG_{INT} = –28.8 kcal/mol is much more exergonic than that for both $ZnBr_2$ and **$[ZnBr_2(ACN)_2]$**, strongly suggesting that *mer*-**$[Zn(Me\text{-}bpa)]^{2+}$** is very likely to form. However, while adding subsequent ACN molecules into Zn coordination in **$[Zn(Me\text{-}bpa)]^{2+}$** diminishes its stability, the addition of Br^{-} anions has the effect of promoting the stability of the formed complex, clearly indicating that the most favorable structure will be **$[ZnBr_2(Me\text{-}bpa)]$** in *mer* conformation with ΔG_{INT} = –47.7 kcal/mol, being 1.5 kcal/mol more stable than the matching *fac* conformation. This is in full agreement with our experimental results, which revealed penta-coordinated *mer*-**$[ZnBr_2(L1)]$** in the solid state. We note in passing that adding the third Br^{-} to the sixth Zn-coordination site results in reducing the stability of the formed system, and is a general feature in all studied complexes.

Replacing **Me-bpa** with the more rigid **Me-terpy** ligand enables only *mer* complexes, as *fac* isomers spontaneously rearrange to *mer* during geometry optimization. Their stabilities are, as a rule, lower compared to the corresponding **$[Zn(Me\text{-}bpa)]^{2+}$** complexes, which is easily rationalized by two synergic effects: (a) the higher flexibility of the **Me-bpa** ligand, which allows more optimal alignment, and (b) the higher intrinsic nucleophilicity of amine nitrogens over pyridines. The latter is nicely evident by analyzing the stability of 1:1 Zn^{2+} complexes with some simple amines and pyridines, **Table 2**. It turns out that, out of five investigated systems, tertiary amine NMe_3 forms strongest complex with Zn^{2+} (ΔG_{INT} = –14.0 kcal/mol), being 2.7 and 4.1 kcal/mol more stable than those with *p*-Me-pyridine and pyridine – a trend that is easily explained by the corresponding pK_a values of these ligands in acetonitrile, declining in the same order (**Table 2**). Therefore, it is reasonable to expect that **Me-deta** will produce the strongest 1:1 complexes with Zn^{2+},

which is, indeed, revealed in **Table 2**. This ligand forms both *mer* and *fac* isomers, with the former always being stable for few kcals/mol. The stability of **[ZnBr$_2$(Me-deta)]** complex is ΔG_{INT} = –49.9 kcal/mol, and is not matched by any 1:1 complex studied here, being 2.2 kcal/mol more stable than **[ZnBr$_2$(Me-bpa)]**.

The **Me-bpa** ligand forms all three 2:1 complexes with Zn^{2+} in solution, **Table 2**. The most stable is *mer* isomer with ΔG_{INT} = –38.3 kcal/mol, but it is closely followed with *cis-fac* having ΔG_{INT} = –36.7 kcal/mol, suggesting that under normal condition the latter will form with around 7% probability. As expected, replacing **Me-bpa** with **Me-terpy** gives only *mer*-**[Zn(Me-terpy)$_2$]$^{2+}$**, which is more stable than its **[Zn(Me-bpa)$_2$]$^{2+}$** counterpart. This is traced down to a fact that the rigid framework of the terpyridine in **Me-terpy** is basically planar, and it practically imposes no steric interference when two such ligands are positioned around Zn^{2+} in *mer* conformation, unlike with **Me-bpa**, where the –CH_2–N(Me)–CH_2– fragment connecting two pyridine units prevents efficient complexation due to its steric requirements. Ligand **Me-deta** follows the trend observed for 1:1 complexes, providing the most stable complexes culminating with *mer*-**Zn[Me-deta]$_2^{2+}$** having ΔG_{INT} = –45.7 kcal/mol.

It is interesting to relate the calculated ΔG_{INT} values for 1:2 complexes to those for 1:1 systems. The contribution of the second ligand amounts to 33%, ΔG_{INT} = –38.3 kcal/mol calculated for *mer*-**[Zn(Me-bpa)$_2$]$^{2+}$** in comparison to ΔG_{INT} = –28.8 kcal/mol obtained for *mer*-**[Zn(Me-bpa)]$^{2+}$**, suggesting that sequential complexation is not cooperative due to steric requirements of the **Me-bpa** ligand. The contribution of the second ligand is 56% in the corresponding *mer* **Me-terpy** complex and 41.5% in the corresponding *mer* **Me-deta** complex. In addition, the calculated ΔG_{INT} values for all three **[Zn(Me-bpa)$_2$]$^{2+}$** complexes are found between –36.3 and –38.3 kcal/mol, being significantly higher than ΔG_{INT} = –47.7 and –46.1 kcal/mol obtained for *mer*- and *fac*-**[ZnBr$_2$(Me-bpa)]** systems, respectively. This provides strong evidence that the presence of two equivalents of strongly nucleophilic Br^- anions will prevent the formation of 1:2 **[Zn(ligand)$_2$]$^{2+}$** complexes and will predominantly result in **[ZnBr$_2$(ligand)]** systems. This finding is in excellent agreement with experimental results reported herein for the ligand **L2**, where the corresponding *mer*-**[ZnBr$_2$(L2)]** complex (**1b**) was isolated and characterized by X-ray single crystal analysis, while the matching 1:2 complex with Br^- as counter-ion could not be isolated, but rather required the use of the non-nucleophilic tetrafluoroborate counter-anion.

Conclusions

In this paper, the synthesis of five amino acid or amine substituted tridentate nitrogen ligands **L1** - **L5** based on the bis(2-picolyl)amine (**bpa**) or bis(2-quinaldyl)amine (**bqa**) framework has been reported. Metal complexes with $Zn(NO_3)_2$, $ZnBr_2$ or $M(NO_3)_2$ in the presence of $Na(BF_4)_2$, M = Zn, Co or Ni, have been prepared, isolated and characterized by ^{1}H, ^{13}C NMR spectroscopy and X-ray single crystal analysis. In particular, the eleven investigated metal complexes can be divided into three groups, namely coordination polymers **(ML)$_n$** (**1p**, **2p**), **ML** complexes (**1n**, **1b**, **2n**, **3n**, **4n**, **5n**) and **ML$_2$** complexes (**1$_2$Zn**, **1$_2$Co**, **1$_2$Ni**). Coordination polymers **1n** or **2n** were formed after hydrolysis of the methyl ester group in the corresponding ligands **L1** or **L2**, respectively. **ML** complexes were isolated with nitrate or bromide counter-ions, regardless of the applied stoichiometry (metal : ligand = 1:1 or 1:2) or the reaction solvent (methanol or acetonitrile). If the non-coordinating tetrafluoroborate was used as counter-ion,[16] isomorphus *cis-fac* **ML$_2$** complexes with different central metal ions (Zn, Co or Ni) could be isolated.

In addition, DFT calculations have been employed to study the relative stability of the Zn^{2+} complexes in acetonitrile solution. It could be shown that in the absence of the **Me-bpa** ligand, the tetrahedral complex **[ZnBr$_2$(ACN)$_2$]** is the most stable species. If the **Me-bpa** ligand is present, *mer*-**[ZnBr$_2$(Me-bpa)]** is the dominant species, where the nucleophilicity of the bromide counter-ions prevents the binding of the second **Me-bpa** ligand. In the absence of bromide counter-ions, a mixture of *cis-fac*, *trans-fac* and *mer* isomers of **[Zn(Me-bpa)$_2$]$^{2+}$** is obtained, with no obvious preference for one isomer.

Previously, we have studied ferrocene amino acid materials[17] and rhodium complexes of triphenylphosphine amino acid bioconjugates as selective catalysts;[18] both systems feature chiral induction *via* artificial hydrogen bonding pattern (Herrick- or van Staveren conformation). The results described herein are an important step towards *cis-fac*-**[M(Aa-bpa)$_2$]$^{2+}$** complexes, that could form similar artificial hydrogen bonding between chiral amino acid side chains, and are potentially useful in the development of new materials and catalysts.

Experimental

General remarks. Reactions were carried out in ordinary glassware and chemicals were used as purchased from commercial suppliers without further purification. Pure (*S*)-phenylethylamine and (*S*)-naphthylethylamine were used. Reactions were monitored by TLC on Silica Gel 60 F254 plates (Merck) and detected with UV lamp (254 nm). Mass spectra were measured on a HPLC-MS system (Agilent Technologies 1200) coupled with 6410 Triple-Quadrupole mass spectrometer, operating in a positive ESI mode. Elemental analyses for C, H and N were carried out using a Perkin Elmer Model 2400 microanalyzer. NMR spectra were obtained on a Bruker Avance 300 or 600 spectrometers, operating at 300 or 600 MHz for ^{1}H and 75 or 150 MHz for ^{13}C. If not mentioned otherwise, the spectra are recorded at room temperature. Chemical shifts, δ (ppm), indicate a downfield shift from the internal standard, tetramethylsilane, TMS, for ^{1}H NMR or residual solvent signal for ^{13}C NMR (77.16 ppm $CDCl_3$ or 39.52 ppm DMSO-d_6). Coupling constants, *J*, are given in Hz. Infrared spectra were recorded using KBr pellets with a Bruker Alpha FT-IR spectrometer, in the 4000–350 cm^{-1} region.

Ligands, general procedure. 2-Picolylchloride hydrochloride or 2-quinaldylchloride hydrochloride (2.5 eq.), *N*-deprotected amino acid

ester or primary amine (1 eq.), K_2CO_3 (10 eq.), KI (1 eq.) and acetonitrile were refluxed for 3 days. The reaction mixture was allowed to cool to room temperature, the solvent was evaporated in vacuum and the residue suspended in ethyl acetate and filtered. The filtrate was washed with 10% $NaHCO_3$ and brine, the organic layer dried over anhydrous sodium sulfate, filtered and evaporated in vacuum. The crude ligand was purified by column chromatography, 1% → 5% methanol in dichloromethane yielding products in the form of yellow oils, which become red-brown upon standing in air. For this reason, purified ligand samples were stored under nitrogen.

Bpa-CH_2-CH_2-CO_2Me, **L1**. 2-Picolylchloride hydrochloride (1.98 g, 12.1 mmol), H-βAla-OMe × HCl (750 mg, 5.37 mmol), K_2CO_3 (8.73 g, 63.2 mmol), KI (875 mg, 5.27 mmol) and acetonitrile (30 mL). Yield: 774 mg (2.71 mmol, 49%), yellow oil. M_r ($C_{16}H_{19}N_3O_2$) = 285.15. MS (EI, 135 eV): *m/z* 308 [36%, M + Na^+], 286 [100%, M + H^+]. ^{1}H NMR (300 MHz, CD_3CN) *δ* / ppm: 8.48-8.46 (m, 2H, H_{Py-6}), 7.70 (dt, 2H, H_{Py-4}, J_1 = 7.7 Hz, J_2 = 1.8 Hz), 7.48 (d, 2H, H_{Py-3}, *J* = 7.8 Hz), 7.21-7.19 (m, 2H, H_{Py-5}), 3.76 (s, 4H, $H_{Py-\alpha}$), 3.56 (s, 3H, H_{OMe}), 2.82 (t, 2H, H_1, *J* = 7.1 Hz), 2.51 (t, 2H, H_2, *J* = 7.1 Hz). ^{1}H NMR (600 MHz, DMSO-d_6) *δ* / ppm: 8.52-8.51 (m, 2H, H_{Py-6}), 7.80 (dt, 2H, H_{Py-4}, J_1 = 7.6 Hz, J_2 = 2.0 Hz), 7.50 (d, 2H, H_{Py-3}, *J* = 7.8 Hz), 7.28 (ddd, 2H, H_{Py-5}, J_1 = 7.4 Hz, J_2 = 4.9 Hz, J_3 = 1.0 Hz), 3.58 (s, 4H, $H_{Py-\alpha}$), 3.35 (s, 3H, H_{OMe}), 2.80 (t, 2H, H_1, *J* = 7.0 Hz), 2.58 (t, 2H, H_2, *J* = 7.0 Hz). ^{13}C NMR (75 MHz, CD_3CN) *δ* / ppm: 173.6, 160.6, 149.7, 137.3, 123.9, 123.0, 60.8, 51.9, 50.6, 33.3.

Bpa-CH_2-CO_2Me, **L2**. 2-Picolylchloride hydrochloride (853 mg, 5 mmol), H-Gly-OMe × HCl (253 mg, 2 mmol), K_2CO_3 (3.32 g, 24 mmol), KI (334 mg, 2 mmol), acetonitrile (50 mL). Yield: 209 mg (0.77 mmol, 38%). M_r ($C_{14}H_{17}N_3O_2$) = 271.31. MS (EI, 135 eV): *m/z* 294 [8%, M + Na^+], 272 [100%, M + H^+], 212 [47%, $M^+ - CO_2Me$], 179 [12%, $M^+ - CH_2Py$], 121 [9%, $PyCH_2NHCH_2^+$]. ^{1}H NMR (600 MHz, $CDCl_3$) *δ* / ppm: 8.53 (d, 2H, H_{Py-6}), 7.67-7.63 (m, 2H, H_{Py-4}), 7.55 (d, 2H, H_{Py-3}, *J* = 7.8 Hz), 7.17-7.13 (m, 2H, H_{Py-5}), 4.00 (s, 4H, $H_{Py-\alpha}$), 3.73 (s, 2H, H_1), 3.70 (s, 3H, H_{OMe}). ^{1}H NMR (300 MHz, CD_3CN) *δ* / ppm: 8.49-8.46 (m, 2H, H_{Py-6}), 7.70 (td, 2H, H_{Py-4}, J_1 = 7.5 Hz, J_2 = 2.0 Hz), 7.52 (d, 2H, H_{Py-3}, *J* = 8.0 Hz), 7.22-7.17 (m, 2H, H_{Py-2}), 3.93 (s, 4H, $H_{Py-\alpha}$), 3.63 (s, 3H, H_{OMe}), 3.42 (s, 2H, H_1). ^{13}C NMR (75 MHz, CD_3CN) *δ* / ppm: 172.53, 160.36, 149.90, 123.97, 123.11, 60.69, 55.31, 51.89.

Bqa-CH_2-CO_2Me, **L3**. 2-Quinaldylchloride hydrochloride (1.07 g, 5 mmol), H-Gly-OMe × HCl (253 mg, 2 mmol), K_2CO_3 (3.32 g, 24 mmol), KI (334 mg, 2 mmol), acetonitrile (50 mL). Yield: 297 mg (0.8 mmol, 40%). M_r ($C_{23}H_{21}N_3O_2$) = 371.43. MS (EI, 135 eV): *m/z* 394 [4%, M + Na^+], 372 [100%, M + H^+], 229 [35%, $M^+ - CH_2Qn$], 142 [12%, $QnCH_2^+$]. ^{1}H NMR (300 MHz, $CDCl_3$) *δ* / ppm: 8.13 (d, 2H, H_{Qn-8}, *J* = 8.6 Hz), 8.05 (d, 2H, H_{Qn-4}, *J* = 8.6 Hz), 7.87 (d, 4H, H_{Qn-5} + H_{Qn-7}, *J* = 8.4 Hz), 7.68 (t, 2H, H_{Qn-6}, *J* = 7.2 Hz), 7.50 (t, 2H, H_{Qn-3}, *J* = 7.2 Hz), 4.18 (s, 4H, $H_{Qn-\alpha}$), 3.69 (s, 3H, H_{OMe}), 3.56 (s, 2H, H_1). ^{1}H NMR (300 MHz, CD_3CN) *δ* / ppm: 8.21 (d, 2H, H_{Qn-8}, *J* = 8.5 Hz), 7.95 (d, 2H, H_{Qn-4}, *J* = 8.5 Hz), 7.87 (dd, 2H, H_{Qn-5}, J_1 = 8.0 Hz, J_2 = 1.0 Hz), 7.75-7.67 (m, 4H, H_{Qn-7} + H_{Qn-6}), 7.56-7.51 (m, 2H, H_{Qn-3}), 4.14 (s, 4H, $H_{Qn-\alpha}$), 3.63 (s, 3H, H_{OMe}), 3.53 (s, 2H, H_1). ^{13}C NMR (75 MHz, CD_3CN) *δ* / ppm: 172.5, 161.1, 148.5, 137.2, 130.3, 129.8, 128.7, 128.4, 127.2, 122.3, 61.6, 55.6, 51.9.

Bpa-CH(CH_3)Ph, **L4**. 2-Picolylchloride hydrochloride (2.0 g, 12.1 mmol), (*S*)-phenylethylamine (515 µL, 4.05 mmol), K_2CO_3 (6.0 g, 43.4 mmol), KI (204 mg, 1.23 mmol), acetonitrile (40 mL). Yield: 690 mg (2.27 mmol, 56%). M_r ($C_{20}H_{21}N_3$) = 303.40. MS (EI, 135 eV): *m/z* 326 [8%, M + Na^+], 304 [78%, M + H^+], 200 [100%, Bpa + H^+], 105 [15%, M^+ – Bpa]. ^{1}H NMR (300 MHz, CD_3CN) *δ* / ppm: 8.43 (ddd, 2H, H_{Py-6}, J_1 = 4.8 Hz, J_2 = 1.6 Hz, J_3 = 0.9 Hz), 7.67 (dt, 2H, H_{Py-4}, J_1 = 7.6 Hz, J_2 = 1.8 Hz), 7.56 (d, 2H, H_{Ph}, *J* = 7.8 Hz), 7.49-7.46 (m, 2H, H_{Py-3}), 7.37 (m, 2H, H_{Ph}), 7.37-7.32 (m, 1H, H_{Ph}), 7.15 (ddd, 2H, H_{Py-5}, J_1 = 7.3 Hz, J_2 = 5.0 Hz, J_3 = 1.2 Hz), 3.92 (q, 1H, H_1, *J* = 6.8 Hz), 3.84 (d, 2H, $H_{Py-\alpha}$, *J* = 14.7 Hz), 3.63 (d, 2H, $H_{Py-\alpha}$, *J* = 14.7 Hz), 1.43 (d, 3H, H_{Me}, *J* = 6.8 Hz). ^{13}C NMR (75 MHz, CD_3CN) *δ* / ppm: 161.6, 149.7, 144.2, 137.3, 129.0, 128.9, 127.9, 123.7, 122.8, 59.6, 57.3, 15.9.

Bqa-CH(CH_3)Nph, **L5**. 2-Quinaldylchloride hydrochloride (1.07 g, 5 mmol), (*S*)-1-naphthylethylamine (320 µL, 2 mmol), K_2CO_3 (3.32 g, 24 mmol), KI (332 mg, 2 mmol), acetonitrile (50 mL). Yield: 822 mg (1.81 mmol, 91%). M_r ($C_{32}H_{27}N_3$) = 453.58. MS (EI, 135 eV): *m/z* 454 [100%, M + H^+], 300 [45%, Bqa], 155 [45%, M^+ – Bqa]. ^{1}H NMR (300 MHz, DMSO-d_6) *δ* / ppm: 8.23 (d, 1H, H_{Qy-8}, *J* = 8.5 Hz), 7.97-7.82 (m, 5H, H_{Ar}), 7.78-7.70 (m, 4H, H_{Ar}), 7.68-7.60 (m, 2H, H_{Ar}), 7.52-7.35 (m, 5H, H_{Ar}), 7.24 (d, 2H, H_{Ar}, *J* = 8.5 Hz), 4.94 (q, 1H, H_1, *J* = 6.7 Hz), 4.05 (m, 4H, $H_{Qn-\alpha}$), 1.67 (d, 3H, H_{Me}). ^{13}C NMR (75 MHz, DMSO-d_6) *δ* / ppm: 160.5, 146.8, 138.9, 135.9, 133.5, 131.6, 129.3, 128.5, 128.4, 127.6, 126.7, 126.0, 125.44, 125.37, 125.1, 124.9, 124.7, 121.2, 57.4, 55.8, 48.6, 13.8.

Metal complexes (**ML**) and **coordination polymers (ML)$_n$**, general procedure. Solutions of the ligand in methanol (5 mL) and the metal salt in methanol (5 mL) were heated and boiled shortly in separate beakers (< 2 min.). Then the metal solution was slowly added to the ligand solution. The reaction mixture was allowed to cool to room temperature and filtered (white ribbon) into a vial (20 mL). After the indicated period, the crystalline product was filtered, washed with diethyl ether (3 × 5 mL) and dried in vacuum.

[Zn(NO_3)$_2$(L1)], **1n**. Ligand **L1** (65 mg, 0.23 mmol), Zn(NO_3)$_2$ × 4 H_2O (57 mg, 0.22 mmol). The vial was placed in a screw capped container (250 mL) filled with diethyl ether (10mL) and left at room temperature. After one day the ether diffused in the vial didn't cause precipitation and the vial was partly covered and left in the fume hood for slow evaporation at room temperature. After several hours, a precipitate occurred. Yield: 55 mg (0.12 mmol, 40%) of colorless solid. ^{1}H NMR (600 MHz, CD_3CN) *δ* / ppm: 8.67 (d, 2H, H_{Py-6}, *J* = 5.2 Hz), 8.06 (dt, 2H, H_{Py-4}, J_1 = 7.7 Hz, J_2 = 1.7 Hz), 7.59-7.57 (m, 2H, H_{Py-3}), 7.52 (d, 2H, H_{Py-5}, *J* = 7.9 Hz), 4.23 (d, 2H, $H_{Py-\alpha}$, *J* = 16.1 Hz), 4.06 (d, 2H, $H_{Py-\alpha}$, *J* = 16.1 Hz), 3.55 (s, 3H, H_{OMe}), 2.95 (t, 2H, H_1, *J* = 7.6 Hz), 2.53 (t, 2H, H_2, *J* = 7.4 Hz). ^{1}H NMR (600 MHz, DMSO-d_6) *δ* / ppm: 8.66 (d, 2H, H_{Py-6}, *J* = 4.8 Hz), 8.13 (dt, 2H, H_{Py-4}, J_1 = 7.8 Hz, J_2 = 1.3 Hz), 7.63-7.61 (m, 2H, H_{Py-3}), 7.57 (d, 2H, H_{Py-5}, *J* = 7.8 Hz), 4.30 (d, 2H, $H_{Py-\alpha}$, *J* = 16.2 Hz), 4.00 (d, 2H, $H_{Py-\alpha}$, *J* = 16.2 Hz), 3.64 (s, 3H, H_{OMe}), 2.96-2.93 (m, 2H, H_1), 2.76-2.74 (m, 2H, H_2). ^{13}C NMR (75 MHz, CD_3CN) *δ* / ppm: 172.7, 155.8, 149.3, 142.2, 126.1, 125.6, 57.4, 52.5, 49.7, 29.0. IR (KBr) *ν* / cm^{-1}: 3076, 3037,

2954, 2918, 2850, 1729, 1608, 1476, 1445, 1384, 1317, 1293, 1211, 1103, 1028, 782, 735, 652, 420.

Alternatively, **1n** was prepared using two other synthetic protocols. **Method B**, 2:1 ligand to metal stoichiometry: Ligand **L1** (69 mg, 0.24 mmol), $Zn(NO_3)_2 \times 4\ H_2O$ (31.7 mg, 0.12 mmol). Volume of the reaction mixture was reduced by evaporation in vacuum (to 2 mL), the vial was placed in a screw capped container (250 mL) filled with diethyl ether (10 mL) and left at room temperature for two weeks. Yield: 23.8 mg (0.05 mmol, 41.5%) of colorless solid. **Method C**, acetonitrile as solvent: Ligand **L1** (66 mg, 0.23 mmol), $Zn(NO_3)_2 \cdot \times 4\ H_2O$ (60.2 mg, 0.23 mmol) and acetonitrile (5+5 mL). The vial was placed in a screw capped container (250 mL) filled with diethyl ether (10 mL) and left at room temperature for one month. Yield 56 mg (0.12 mmol, 49%).

Methyl ester group in complexes **1n** and **2n** hydrolyzes to acid upon standing in DMSO solution, which was proven for **1n** by comparison of newly formed peaks with spectra of complex **$[Zn(NO_3)(Bpa\text{-}(CH_2)_2CO_2)]$** known from the literature.[4d]

$[ZnBr_2(L1)]$, **1b**. Ligand **L1** (66 mg, 0.23 mmol), $ZnBr_2$ (52 mg, 0.23 mmol). The vial was partly covered and left in the fume hood for slow evaporation at room temperature for two days. Yield: 67 mg (0.13 mmol, 57%) of colorless crystals, suitable for X-ray single crystal analysis. Elemental analysis calcd (%) for $C_{16}H_{19}Br_2N_3O_2Zn$: C 37.64, H 3.75, N 8.23. Found: C 37.71, H 3.44, N 8.19. ^{1}H NMR (600 MHz, CD_3CN) δ / ppm: 9.07 (d, 2H, $H_{Py\text{-}6}$, J = 4.9 Hz), 8.01 (dt, 2H, $H_{Py\text{-}4}$, J_1 = 7.7 Hz, J_2 = 1.7 Hz), 7.58 (m, 2H, $H_{Py\text{-}3}$, J = 6.2 Hz), 7.47 (d, 2H, $H_{Py\text{-}5}$, J = 7.8 Hz), 4.22 (s, 4H, $H_{Py\text{-}\alpha}$), 3.49 (s, 3H, H_{OMe}), 2.86-2.83 (m, 2H, H_1), 2.43-2.41 (m, 2H, H_2). ^{1}H NMR (600 MHz, CD_3CN, -40 °C) δ / ppm: 9.02 (d, 2H, $H_{Py\text{-}6}$, J = 4.9 Hz), 8.01 (dt, 2H, $H_{Py\text{-}4}$, J_1 = 7.7 Hz, J_2 = 1.7 Hz), 7.58 (t, 2H, $H_{Py\text{-}3}$, J = 6.2 Hz), 7.46 (d, 2H, $H_{Py\text{-}5}$, J = 7.8 Hz), 4.22 (d, 2H, $H_{Py\text{-}\alpha}$, J = 16.0 Hz), 4.18 (d, 2H, $H_{Py\text{-}\alpha}$, J = 16.0 Hz) 3.43 (s, 3H, H_{OMe}), 2.77 (t, 2H, H_1, J = 7.6 Hz), 2.39 (t, 2H, H_2, J = 7.6 Hz). ^{1}H NMR (600 MHz, DMSO-d_6) δ / ppm: 8.89 (br s, 2H, $H_{Py\text{-}6}$), 8.12 (br s, 2H, $H_{Py\text{-}4}$), 7.67 (br s, 2H, $H_{Py\text{-}3}$), 7.64 (d, 2H, $H_{Py\text{-}5}$, J = 7.6 Hz), 4.29-4.05 (br s, 4H, $H_{Py\text{-}\alpha}$), 3.52 (s, 3H, H_{OMe}), 2.89 (t, 2H, H_1, J = 7.4 Hz), 2.58-2.55 (m, 2H, H_2). ^{13}C NMR (75 MHz, CD_3CN) δ / ppm: 172.4, 154.6, 149.3, 141.3, 125.5, 124.9, 57.8, 52.3, 49.1, 29.7. IR (KBr) ν / cm^{-1}: 3071, 3028, 2952, 2917, 2850, 1734, 1481, 1442, 1292, 1204, 1103, 1049, 1020, 782, 765, 463, 418.

Alternatively, **1b** was prepared using two other synthetic protocols. **Method B**, 2:1 ligand to metal stoichiometry: Ligand **L1** (60 mg, 0.21 mmol), $ZnBr_2$ (24 mg, 0.1 mmol). Volume of the reaction mixture was reduced by evaporation in vacuum (to 2 mL), the vial was placed in a screw capped container (250 mL) filled with diethyl ether (10 mL) and left at room temperature for two days. Yield: 26.4 mg (0.05 mmol, 51.7%). **Method C**, acetonitrile as solvent: Ligand **L1** (65 mg, 0.23 mmol), $ZnBr_2$ (52.5 mg, 0.23 mmol) and acetonitrile (5+5 mL). The vial was placed in a screw capped container (250 mL) filled with diethyl ether (10 mL) and left at room temperature for one month. Yield: 75 mg (0.15 mmol, 70%).

$[Zn(L2)(NO_3)_2]$, **2n**. Ligand **L2** (57 mg, 0.2 mmol), $Zn(NO_3)_2 \times 4\ H_2O$ (27 mg, 0.1 mmol). Volume of the reaction mixture was reduced by evaporation in vacuum (to 2 mL), the vial was placed in a screw capped container (250 mL) filled with diethyl ether (10 mL) and left at room temperature for one day. Yield: 34 mg (0.074 mmol, 73%), crystals suitable for X-ray single crystal analysis. Elemental analysis calcd (%) for $C_{15}H_{17}N_5O_8Zn$: C 39.10, H 3.72, N 15.20. Found: C 39.09, H 3.64, N 14.92. ^{1}H NMR (600 MHz, CD_3CN) δ / ppm: 8.69 (d, 2H, $H_{Py\text{-}6}$, J = 5.0 Hz), 8.07 (td, 2H, $H_{Py\text{-}4}$, J_1 = 8 Hz, J_2 = 1.5 Hz), 7.62-7.55 (m, 2H, $H_{Py\text{-}3}$), 7.56 (d, 2H, $H_{Py\text{-}5}$, J = 7.8 Hz), 4.56 (d, 2H, $H_{Py\text{-}\alpha}$, J = 16.5 Hz), 4.33 (d, 2H, $H_{Py\text{-}\alpha}$, J = 16.5 Hz), 3.68 (s, 3H, H_{OMe}), 3.46 (s, 2H, H_1). ^{13}C NMR (150 MHz, CD_3CN) δ / ppm: 170.18, 154.27, 147.34, 140.54, 124.73, 124.65, 64.92, 59.92, 57.84, 54.96, 51.91. IR (KBr) ν / cm^{-1}: 3103, 3073, 2957, 2942, 1748, 1609, 1467, 1385, 1314, 1295, 1219, 1134, 1102, 1058, 1028, 983, 819, 768, 721, 652, 506, 473, 419.

$[Zn(NO_3)_2(L3)]$, **3n**. Ligand **L3** (47 mg, 0.126 mmol), $Zn(NO_3)_2 \times 4\ H_2O$ (15 mg, 0.057 mmol). The vial was partly covered and left in the fume hood for slow evaporation at room temperature for 1 h. Yield: 28 mg (0.05 mmol, 40%), crystals suitable for X-ray single crystal analysis. Elemental analysis calcd (%) for $C_{23}H_{21}N_5O_8Zn$: C 49.26, H 3.77, N 12.49. Found: C 49.10, H 3.58, N 12.49. ^{1}H NMR (600 MHz, CD_3CN) δ / ppm: 8.63 (d, 2H, $H_{Qn\text{-}8}$, J = 8.5 Hz), 8.59 (d, 2H, $H_{Qn\text{-}4}$, J = 8.5 Hz), 8.09 (d, 2H, $H_{Qn\text{-}5}$, J = 8.0 Hz), 8.01-7.99 (m, 2H, $H_{Qn\text{-}7}$), 7.77-7.75 (m, 2H, $H_{Qn\text{-}6}$), 7.60 (d, 2H, $H_{Qn\text{-}3}$, J = 8.5 Hz), 5.07 (d, 2H, $H_{Qn\text{-}\alpha}$, J = 17.0 Hz), 4.63 (d, 2H, $H_{Qn\text{-}\alpha}$, J = 17.0 Hz), 3.81 (s, 2H, H_1), 3.69 (s, 3H, H_{OMe}). ^{13}C NMR (150 MHz, DMSO) δ / ppm: 171.1, 159.8, 146.2, 136.5, 129.5, 128.6, 127.8, 126.2, 121.1, 59.9, 54.4, 51.2. IR (KBr) ν / cm^{-1}: 3068, 3010, 2962, 2928, 1742, 1620, 1598, 1514, 1466, 1385, 1300, 1222, 1119, 1092, 1028, 963, 899, 829, 785, 748, 635, 487, 405.

$[Zn(NO_3)_2(L4)]$, **4n**. Ligand **L4** (61 mg, 0.2 mmol), $Zn(NO_3)_2 \times 4\ H_2O$ (53 mg, 0.2 mmol). The vial was partly covered and left in the fume hood for slow evaporation at room temperature for several hours. Yield: 34 mg (0.069 mmol, 35%), crystals suitable for X-ray single crystal analysis. Elemental analysis calcd (%) for $C_{20}H_{21}N_5O_6Zn$: C 48.74, H 4.30, N 14.21. Found: C 48.58, H 4.13, N 14.27. ^{1}H NMR (600 MHz, CD_3CN) δ / ppm (broad peaks at room temperature): 8.73 (s, 2H, H_{Ar}), 8.10-7.99 (m, 2H, H_{Ar}), 7.63-7.56 (m, 2H, H_{Ar}), 7.45 (d, 2H, H_{Ar}, J = 8.0 Hz), 7.39-7.32 (m, 5H, H_{Ar}), 4.56 (d, 1H, $H_{Py\text{-}\alpha}$, J = 17.0 Hz), 4.17 (d, 1H, $H_{Py\text{-}\alpha}$, J = 16.0 Hz), 4.11 (q, 1H, H_1, J = 7.0 Hz), 3.80 (d, 2H, $H_{Py\text{-}\alpha}$, J = 16.0 Hz), 1.34 (d, 3H, H_{Me}, J = 7.0 Hz). ^{13}C NMR (150 MHz, DMSO-d_6) δ / ppm: 156.45, 154.72, 148.03, 147.44, 140.89, 137.87, 129.24, 128.54, 128.45, 124.80, 124.42, 124.05, 62.19, 57.81, 52.12, 18.92. IR (KBr) ν / cm^{-1}: 3114, 3038, 2983, 2906, 1609, 1477, 1453, 1426, 1323, 1293, 1103, 1023, 821, 776, 749, 702, 652, 533, 415.

$[Zn(NO_3)_2(L5)]$, **5n**. Ligand **L5** (101 mg, 0.22 mmol), $Zn(NO_3)_2 \times 4\ H_2O$ (29 mg, 0.1 mmol). The vial was partly covered and left in the fume hood for slow evaporation at room temperature for 1 day. Yield 21 mg (0.03 mmol, 13%), crystals suitable for X-ray single crystal analysis. Elemental analysis calcd (%) for $C_{32}H_{27}N_5O_6Zn$: C 59.78, H 4.23, N 10.89. Found: C 59.54, H 4.60, N 10.81. ^{1}H NMR (300 MHz, DMSO-d_6) δ / ppm: 8.22 (d, 1H, H_{Ar}, J = 8.5 Hz), 8.11 (d, 2H, H_{Ar}, J = 8.5 Hz), 7.95-7.63 (m, 9H, H_{Ar}), 7.55-7.34 (m, 5H, H_{Ar}), 7.29 (d, 2H, H_{Ar} J = 8.5 Hz), 4.89 (q, 1H, H_1, J_1 = 7 Hz, J_2 = 6.5 Hz), 4.03 (q, 4H, $H_{Qn\text{-}\alpha}$, J = 15.0 Hz), 1.61 (d, 3H, H_{Me}, J = 6.5 Hz). ^{13}C NMR (150 MHz, DMSO-d_6) δ / ppm: 160.5, 146.8, 138.9, 135.9, 133.6,

Table 3. Experimental data for the X–ray diffraction studies.

	1p	**2p**	**1b**	**2n**	**3n**
formula	$C_{17}H_{20}N_4O_{5.5}Zn$	$C_{30}H_{35}N_9O_{12}Zn_2$	$C_{16}H_{19}Br_2N_3O_2Zn$	$C_{15}H_{17}N_5O_8Zn$	$C_{23}H_{21}N_5O_8Zn$
Fw (g mol^{-1})	433.74	844.41	510.53	460.71	560.82
crystal size (mm)	0.25 × 0.15 × 0.15	0.25 × 0.05 × 0.03	0.28 × 0.15 × 0.03	0.25 × 0.10 × 0.05	0.30 × 0.10 × 0.05
crystal color	colorless	colorless	colorless	light yellow	colorless
crystal system	monoclinic	monoclinic	triclinic	triclinic	monoclinic
space group	*C*2/*c*	*P*2$_1$/*n*	*P*–1	*P*–1	*P*2$_1$/*n*
a (Å)	26.1564(6)	9.5678(2)	7.5873(7)	8.0542(5)	13.9549(4)
b (Å)	7.8711(2)	23.4648(7)	8.5099(8)	8.5048(6)	12.2190(4)
c (Å)	21.2024(5)	15.4587(5)	17.2513(13)	16.0539(8)	14.9510(4)
α (º)	90	90	79.837(6)	84.712(5)	90
β (º)	121.9020(10)	92.616(2)	85.822(5)	86.468(5)	111.883(2)
γ (º)	90	90	67.110(4)	77.287(5)	90
V (Å^3)	3705.80(15)	3466.96(17)	1010.04(15)	1067.2(10)	2365.68(12)
Z	8	4	2	2	4
$D_{calc.}$ (g cm^{-3})	1.555	1.618	1.679	1.434	1.575
F(000)	1792	1736	504	472	1152
Reflns collected	7358	15111	4775	9529	9960
Independ. reflns	4221	7935	3358	4345	5374
R_{int}	0.0202	0.0448	0.0405	0.0479	0.0426
Reflns observed	3552	5754	2553	3931	3115
Parameters	250	491	218	263	335
$R[I > 2\sigma(I)]^a$	0.0313	0.0501	0.0480	0.0749	0.0587
wR_2 (all data)^b	0.0807	0.1954	0.1263	0.2433	0.1446
Goof , S^c	1.049	1.173	1.092	1.135	1.015
maximum/minimum residual electron density (e Å^{-3})	+0.92/–0.39	+0.86/–0.90	+0.48/–0.67	+2.23/–0.50	+0.86/–0.69

^{a} $R = \sum||F_o| - |F_c||/\sum|F_o|$. ^{b} $wR_2 = \{\sum[w(F_o^2 - F_c^2)^2]/\sum[w(F_o^2)^2]\}^{1/2}$. ^{c} $S = \{\sum[w(F_o^2 - F_c^2)^2]/(n/p)\}^{1/2}$ where *n* is the number of reflections and *p* is the total number of parameters refined.

131.6, 129.3, 128.5, 128.4, 127.6, 126.7, 126.0, 125.44, 125.37, 125.1, 124.9, 124.7, 121.2, 57.4, 55.8, 13.9. IR (KBr) ν / cm^{-1}: 3062, 2987, 2933, 1620, 1600, 1514, 1469, 1384, 1292, 1025, 831, 772, 746, 629, 406.

[Zn(L1)]NO$_3$ × Et$_2$O]$_n$, **1p**. Ligand **L1** (36.0 mg, 0.126 mmol), $Zn(NO_3)_2 \times 4\ H_2O$ (15 mg, 0.057 mmol). The vial was place in a tank (250 ml) filled with diethyl ether (10 ml) for diffusion. Since no crystallization occurred, the vial was left at room temperature for evaporation to dryness; a very small amount of crystals suitable for X-ray single crystal analysis was formed.

{[Zn(BpaCH$_2$CO$_2$)][Zn(BpaCH$_2$CO$_2$)(H$_2$O)]}$_n$ (NO$_3$)$_{2n}$ × (H$_2$O)$_n$ × (CH$_3$CN)$_n$, **2p**. Ligand **L2** (34.2 mg, 0.126 mmol), $Zn(NO_3)_2 \times 4\ H_2O$ (15 mg, 0.057 mmol). The vial was placed in a tank (250 ml) filled with diethyl ether (10 ml) for diffusion. Since no crystallization occurred, the vial was left at room temperature for evaporation to dryness; a very small amount of crystals suitable for X-ray single crystal analysis formed.

Metal complexes (**ML$_2$**), general procedure. Solutions of the ligand in methanol (5 mL) and the metal salt in methanol (5 mL) were heated to shortly boiling in separate beakers (< 2 min.). Then the metal solution was slowly added to the ligand solution. To this solution, $NaBF_4$ in methanol (2 mL) was added; the volume was reduced by evaporation in vacuum (~5 mL). After the indicated period, crystals appeared. The solvent was decanted and the crystals were washed with diethyl ether (3 × 5 mL) and dried in vacuum.

[Zn(L1)$_2$](BF$_4$)$_2$, **1$_2$Zn**. Ligand **L1** (107 mg, 0.38 mmol), $Zn(NO_3)_2 \times 4\ H_2O$ (49 mg, 0.19 mmol), $NaBF_4$ (84 mg, 0.38 mmol) in methanol (4 mL). The vial was left for several hours in the refrigerator (at 4 °C). Yield: 124 mg (0.16 mmol, 82%) of colorless crystals, suitable for X-ray single crystal analysis. Elemental analysis calcd (%) for $C_{32}H_{38}B_2F_8N_6O_4Zn$: C 47.47, H 4.73, N 10.38. Found: C 47.31, H 4.71, N 10.76. ^{1}H NMR (300 MHz, CD_3CN) and ^{13}C NMR (75 MHz, CD_3CN) revealed very broad signals at room temperature; ^{1}H NMR (600 MHz, CD_3CN, -40 °C) δ / ppm: 8.66 (d, 2H, $H_{Py\text{-}6}$, J = 5.0 Hz), 8.19 (dt, 2H, $H_{Py\text{-}4}$, J_1 = 7.8 Hz, J_2 = 1.4 Hz), 8.02 (dt, 2H, $H_{Py\text{-}4'}$, J_1 = 7.8 Hz, J_2 =

Table 4. Experimental data for the X–ray diffraction studies.

	4n	**5n**	**1_2Zn**	**1_2Co**	**1_2Ni**
formula	$C_{20}H_{21}N_5O_6Zn$	$C_{32}H_{27}N_5O_6Zn$	$C_{32}H_{38}B_2F_8N_6O_4Zn$	$C_{32}H_{38}B_2CoF_8N_6O_4$	$C_{32}H_{38}B_2F_8N_6NiO_4$
Fw (g mol^{-1})	492.79	642.96	809.67	803.23	803.01
crystal size (mm)	0.15 × 0.10 × 0.08	0.20 × 0.10 × 0.10	0.20 × 0.10 × 0.05	0.10 × 0.10 × 0.05	0.25 × 0.18 × 0.15
crystal color	light yellow	colorless	colorless	light pink	blue
crystal system	monoclinic	orthorhombic	orthorhombic	orthorhombic	orthorhombic
space group	$P2_1$	$P2_12_12_1$	*Pbcn*	*Pbcn*	*Pbcn*
a (Å)	7.3797(2)	9.8292(5)	19.3596(3)	19.3097(11)	19.4164(2)
b (Å)	17.4297(3)	11.9795(8)	10.1740(2)	10.1965(5)	10.34210(10)
c (Å)	8.7740(2)	26.3978(17)	18.4718(3)	18.4325(11)	17.9742(2)
α (º)	90	90	90	90	90
β (º)	110.727(3)	90	90	90	90
γ (º)	90	90	90	90	90
V (Å^3)	1055.52(4)	3108.3(3)	3638.29(11)	3629.2(3)	3609.33(6)
Z	2	4	4	4	4
$D_{calc.}$ (g cm^{-3})	1.551	1.374	1.478	1.470	1.478
F(000)	508	1328	1664	1652	1656
Reflns collected	5088	11895	11828	9031	11856
Independent reflns	3475	6562	3766	3604	3712
R_{int}	0.0261	0.0416	0.0188	0.0323	0.0149
Reflns observed	3378	4386	3242	2719	3410
Parameters	290	398	241	241	241
$R[I > 2\sigma(I)]^a$	0.0535	0.0619	0.0345	0.0455	0.0385
wR_2 (all data)^b	0.1482	0.1753	0.1000	0.1275	0.1114
Goof , S^c	1.075	1.018	1.072	1.022	1.076
maximum/minimum residual electron density (e Å^{-3})	+0.54/–0.73	+0.99/–0.30	+0.25/–0.24	+0.25/–0.24	+0.32/–0.24

^{a} $R = \sum||F_o| - |F_c||/\sum|F_o|$. ^{b} $wR_2 = \{\sum[w(F_o^2 - F_c^2)^2]/\sum[w(F_o^2)^2]\}^{1/2}$. ^{c} $S = \{\sum[w(F_o^2 - F_c^2)^2]/(n/p)\}^{1/2}$ where *n* is the number of reflections and *p* is the total number of parameters refined.

1.4 Hz), 7.74 (t, 2H, $H_{Py\text{-}5}$, *J* = 6.4 Hz), 7.60 (d, 2H, $H_{Py\text{-}3}$, *J* = 7.8 Hz), 7.54 (d, 2H, $H_{Py\text{-}3'}$, *J* = 7.8 Hz), 7.35-7.30 (m, 4H $H_{Py\text{-}6'}$ + $H_{Py\text{-}5'}$), 4.30 (d, 2H, $H_{Py\text{-}\alpha}$, *J* = 16.0 Hz), 4.12 (d, 2H, $H_{Py\text{-}\alpha}$, *J* = 16.0 Hz), 3.93 (d, 2H, $H_{Py\text{-}\alpha'}$, *J* = 16.0 Hz), 3.53 (d, 2H, $H_{Py\text{-}\alpha'}$, *J* = 16.0 Hz), 3.48 (s, 6H, H_{OMe}), 2.72-2.63 (m, 2H, H_1), 2.53-2.43 (m, 4H, H_1 + H_2), 2.14-2.06 (m, 2H, H_2). ^{13}C NMR (150 MHz, CD_3CN, -40 °C) *δ* / ppm: 171.8, 156.2, 154.9, 148.7, 148.1, 141.9, 141.3, 126.6, 126.1, 125.8, 125.4, 56.6, 53.7, 51.8, 48.7, 26.1. When the complex **1_2Zn** is dissolved in DMSO-d_6, it dissociates to 1:1 (**M**:**L**) complex and free ligand **L1**, which was proven by comparison of observed ^{1}H and ^{13}C NMR spectra with that of free ligand **L1** and complex **1n** in DMSO-d_6. IR (KBr) ν / cm^{-1}: 3129, 3082, 3045, 3004, 2956, 1734, 1612, 1493, 1449, 1391, 1324, 1200, 1054, 863, 768, 643, 518, 421.

$[Co(L1)_2](BF_4)_2$, **1_2Co**. Ligand **L1** (108 mg, 0.38 mmol), $Co(NO_3)_2$ × 6 H_2O (55 mg, 0.19 mmol), $NaBF_4$ (42 mg, 0.38 mmol) in methanol (2 mL). The vial was partly covered and left in the fume hood at room temperature for two weeks. Yield: 84 mg (0.10 mmol, 55%) of purple crystals, suitable for X-ray single crystal analysis. Elemental analysis calcd (%) for $C_{32}H_{38}B_2CoF_8N_6O_4$: C 47.85, H 4.77, N 10.46. Found: C 47.64, H 4.92, N 10.62. IR (KBr) ν / cm^{-1}: 3122, 3085, 3045, 3004, 2957, 1734, 1610, 1491, 1449, 1391, 1324, 1198, 1054, 861, 768, 644, 521, 423.

$[Ni(L1)_2](BF_4)_2$, **1_2Ni**. Ligand **L1** (86.4 mg, 0.30 mmol), $Ni(NO_3)_2$ × 6 H_2O (44 mg, 0.15 mmol), $NaBF_4$ (34 mg, 0.30 mmol) in methanol (2 mL). The vial was partly covered and left in the fume hood at room temperature for several hours. Yield: 94 mg (0.12 mmol, 59 %) of violet crystals, suitable for X-ray single crystal analysis. Elemental analysis calcd (%) for $C_{32}H_{38}B_2F_8N_6NiO_4$: C 47.86, H 4.77, N 10.47. Found: C 47.60, H 4.94, N 10.60. IR (KBr) ν / cm^{-1}: 3124, 3086, 3045, 3004, 2957, 1735, 1610, 1491, 1449, 1389, 1324, 1198, 1054, 861, 770, 644, 520, 429.

X–ray crystallography. The X–ray intensity data were collected at room temperature on a Nonius Kappa CCD diffractometer equipped with graphite–monochromated Mo–K_α radiation (λ = 0.71073 Å) at room temperature for **1b**, **1p**, **2p** and **3n** or on Agilent SuperNova dual source with Atlas detector equipped with mirror–monochromated Cu–K_α radiation (λ = 1.54184 Å) at room

temperature for **2n**, **4n**, **1_2Zn**, **1_2Co** and **1_2Ni** or Mo–K_α radiation (λ = 0.71073 Å) at room temperature for **5n**. The data were processed using DENZO[19] (**1b**, **1p**, **2p**, **3n**) or CRYSALIS PRO[20] (**2n**, **4n**, **5n**, **1_2Zn**, **1_2Co**, **1_2Ni**). The structures were solved by direct (or Patterson for **1p**) methods using SHELXS-97[21] or SIR-92[22] (**2n** and **5n**) and refined against F^2 on all data by a full–matrix least squares procedure with SHELXL–97.[21] All non–hydrogen atoms were refined anisotropically. All hydrogen atoms bonded to carbon were included in the model at geometrically calculated positions and refined using a riding model. The water hydrogen atoms in **2p** were located in the difference map and refined with the distance restraints (DFIX) with O–H = 0.84 and with U_{iso}(H) = 1.5U_{eq}(O). The figures were prepared using DIAMOND 3.2 software.[23]

The residual density peak was observed in the difference Fourier map of **2n** with the distance to C14 of 3.53 Å. This peak was unrefinable and probably can be attributed to disordered solvent molecule. A potential solvent-accesible volume of 100.8 Å^3 and 173.6 Å^3 was found in the structure of complex **1b** and **2n**, respectively. The empty channels were found in the structure of **2n**, running along the crystallographic *a*-axis.

CCDC reference numbers are 1418408 (**1p**), 1418409 (**2p**), 1418410 (**1b**), 1418411 (**2n**), 1418412 (**3n**), 1418413 (**4n**), 1418414 (**5n**), 1418415 (**1_2Zn**), 1418416 (**1_2Co**), 1418417 (**1_2Ni**). These data can be obtained free of charge from The Cambridge Crystallographic Data Centre *via* www.ccdc.cam.ac.uk/data_request/cif.

Computational details. In order to sample the conformational flexibility of all investigated complexes and unbound ligands, classical *in vacuo* molecular dynamics (MD) simulations were performed employing a standard generalized AMBER force field (GAFF)[24] with atomic charges obtained by the AM1-BCC method[25] as implemented within the AMBER12 program package.[26] The energy minimization was performed in a two-step procedure, initially (1500 steps) minimizing only hydrogen atoms under the harmonic constrain of heavy atoms with the force constant of 32 kcal mol^{-1} Å^{-2}, followed by a relaxed all-atom minimization (2500 steps). Upon gradual heating from 0 K, MD simulations were performed at 400 K for a period of 300 ns, maintaining the temperature constant using the Langevin thermostat with a collision frequency of 1 ps^{-1}. Subsequently, we simulated each system solvated in the box of acetonitrile (ACN) consisting of 210 ACN molecules using the same setup. Up to five most stable distinct structures from both sets of simulations were reoptimized using a very efficient quantum mechanical (QM) M05–2X/6–31+G(d)/LanL2DZ + ECP model, known to be successful in reproducing geometries, dipole moments and homolytic bond energies in various zinc complexes.[27] Thermal Gibbs free energy corrections were extracted from the corresponding frequency calculations and the structures were checked for the absence of imaginary frequencies. The final single-point energies were attained with a highly flexible 6–311++G(2df,2pd) basis set using the M05–2X functional, which was designed by Truhlar's group to provide very accurate thermodynamic parameters, being particularly successful in treating nonbonding interactions.[28] This gives rise to the M05–2X/6–311++G(2df,2pd)//M05–2X/6–31+G(d)/LanL2DZ + ECP model employed here for the gas-phase studies. The influence of acetonitrile as a solvent was included using the implicit SMD solvation model (ε = 35.688) by correcting the latter gas-phase interaction energies with the difference in the optimized (SMD)/M05–2X/6–31+G(d)/LanL2DZ + ECP total electronic energies and the corresponding gas-phase values obtained at the same level of theory. All QM calculations were performed using the Gaussian 09 software.[29] Cartesian coordinates for all computed molecules are collected in a single text file readable by the program Mercury (version 3.3 or later).[30]

Acknowledgements

These materials are based on work financed by the Croatian Science Foundation (HrZZ, project numbers IP-2014-09-1461 and IP-2014-09-3386), Slovenian Research Agency (Grant P1-0175-103), Croatian-Slovenian bilateral project and partly supported through the infrastructure of the EN-FIST Centre of Excellence, Ljubljana. We thank COST Action CM1105 for financial support.

Notes and references

1 (a) C. Wende, C. Lüdtke and N. Kulak, *Eur. J. Inorg. Chem.*, 2014, 2597; (b) D.-L. Ma, H.-Z. He, K.-H. Leung, D. S.-H. Chan and C.-H. Leung, *Angew. Chem. Int. Ed.*, 2013, **52**, 7666; (c) M. R. Gill and J. A. Thomas, *Chem. Soc. Rev.*, 2012, **41**, 3179; (d) L. Salassa, *Eur. J. Inorg. Chem.*, 2011, 4931; (e) U. Schatzschneider, *Eur. J. Inorg. Chem.*, 2010, 1451.

2 (a) R. D. Hancock, *Chem. Soc. Rev.*, 2013, **42**, 1500; (b) J. G. Vos and J. M. Kelly, *Dalton Trans.*, 2006, 4869; (c) J. H. Alstrum-Acevedo, M. K. Brennaman and T. J. Meyer, *Inorg. Chem.*, 2005, **44**, 6802.

3 (a) S. Mortezaei, N. Caterineu and J. W. Canary, *J. Am. Chem. Soc.*, 2012, **134**, 8504; (b) K. Sundaravel, E. Suresh, K. Saminathan and M. Palaniandavar, *Dalton Trans.*, 2011, **40**, 8092; (c) M. Frezza, S. S. Hindo, D. Tomco, M. M. Allard, Q. C. Cui, M. J. Heeg, D. Chen, Q. P. Dou and C. N. Verani, *Inorg. Chem.*, 2009, **48**, 5928; (d) M. J. Carney, N. J. Robertson, J. A. Halfen, L. N. Zakharov and A. L. Rheingold, *Organometallics*, 2004, **23**, 6184; (e) P. R. Andres and U. S. Schubert, *Adv. Mater.*, 2004, **16**, 1043; (f) A. Ojida, Y. Mito-oka, K. Sada and I. Hamachi, *J. Am. Chem. Soc.*, 2004, **126**, 2454.

4 For **[Zn(NO$_3$)$_2$(bpa)]** complexes see: (a) Y. Song, D. Kim, H.-J. Lee, H. Lee, *Inorg. Chem. Commun.*, 2014, **45**, 66; (b) L. Gotzke, K. Gloe, K. A. Jolliffe, L. F. Lindoy, A. Heine, T. Doert, A. Jäger and K. Gloe, *Polyhedron*, 2011, **30**, 708; (c) Y. Kim, B. K. Park, G. H. Eom, S. H. Kim, H. M. Park, Y. S. Choi, H. G. Jang and C. Kim, *Inorg. Chim. Acta*, 2011, **366**, 337; (d) S. I. Kirin, P. Dübon, T. Weyhermüller, E. Bill and N. Metzler-Nolte, *Inorg. Chem.*, 2005, **44**, 5405.

5 For **[ZnX$_2$(bpa)]** complexes see: (a) J. Qian, L. Wang, W. Gu, X. Liu, J. Tian and S. Yan, *Dalton Trans.*, 2011, **40**, 5617; (b) A. Beitat, S. P. Foxon, C.-C. Brombach, H. Hausmann, F. W. Heinemann, F. Hampel, U. Monkowius, C. Hirtenlehner, G. Knor and S. Schindler, *Dalton Trans.*, 2011, **40**, 5090; (c) A. Abufarag and H. Vahrenkamp, *Inorg. Chem.*, 1995, **34**, 2207.

6 For **[Zn(R-bpa)$_2$]$^{2+}$** complexes, R ≠ H, see: (a) J. T. Simmons, Z. Yuan, K. L. Daykin, B. G. Nguyen, R. J. Clark, M. Shatruk and L. Zhu, *Supramol. Chem.*, 2014, **26**, 214; (b) J. T. Simmons, J. R.

Allen, D. R. Morris, R. J. Clark, C. W. Levenson, M. W. Davidson and L. Zhu, *Inorg. Chem.*, 2013, **52**, 5838; (c) B. Maity, S. Gadadhar, T. K. Goswami, A. A. Karande, A. R. Chakravarty, *Dalton Trans.*, 2011, **40**, 11904; (d) Y. Mikata, T. Fujimoto, T. Fujiwara and S. Kondo, *Inorg. Chim. Acta*, 2011, **370**, 420; (e) S. Banthia and A. Samanta, *Eur. J. Org. Chem.*, 2005, 4967.

7 (a) S. I. Kirin, I. Ott, R. Gust, W. Mier, T. Weyhermüller and N. Metzler-Nolte, *Angew. Chem. Int. Ed.*, 2008, **47**, 955; (b) S. I. Kirin, H. P. Yennawar and M. E. Williams, *Eur. J. Inorg. Chem.*, 2007, 3686; (c) S. I. Kirin, C. M. Happel, S. Hrubanova, T. Weyhermüller, C. Klein and N. Metzler-Nolte, *Dalton Trans.*, 2004, 1201.

8 Zn **bpa** complexes are known to be *trans*-eterification catalysts: (a) N. Niklas, A. Zahl and R. Alsfasser, *Dalton Trans.*, 2007, 154; (b) see also reference 4c.

9 A. W. Addison, T. N. Rao, J. Reedijk, J. van Rijn and G. C. Verschoor, *J. Chem. Soc., Dalton Trans*., 1984, 1349.

10 (a) M. Bartholoma, B. Ploier, H. Cheung, W. Ouellette and J. Zubieta, *Inorg. Chim. Acta*, 2010, **363**, 1659; (b) K.-Y. Choi and Y.-M. Jeon, *Main Group Met. Chem.*, 2003, **26**, 313; (c) L.-S. Long, L.-S. Zheng, X.-M. Chen and S. W. Ng, *Main Group Met. Chem*., 2001, **24**, 465; (d) A. Trosch and H. Vahrenkamp, *Eur. J. Inorg. Chem.*, 1998, 827.

11 J. Glerup, P. A. Coodson, D. J. Hodgson, K. Michelsen, K. M. Nielsen and H. Weihe, *Inorg. Chem.*, 1992, **31**, 4611.

12 For representative literature on transition metal complexes of **Me-terpy** and **Me-deta** see: (a) A. Rilak, I. Bratsos, E. Zangrando, J. Kljun, I. Turel, Z. Bugarcic and E. Alessio, *Inorg. Chem.*, 2014, **53**, 6113; (c) E. C. Constable, *Chem. Soc. Rev.*, 2007, **36**, 246; (b) C. H. Lin, S. L. Wang and K. H. Lii, *J. Am. Chem. Soc.*, 2001, **123**, 4649.

13 J. Torras and C. Alemán, *J. Phys. Chem. B*, 2013, **117**, 10513.

14 For an X-ray structure of **$[ZnBr_2(MeCN)_2]$** see: G. Bhosekar, I. Jeβ and C. Näther, *Z. Naturforsch. B, Chem. Sci.*, 2006, **61**, 721.

15 (a) I. Kaljurand, A. Kütt, L. Sooväli, T. Rodima, V. Mäemets, I. Leito and I. A. Koppel, *J. Org. Chem.*, 2005, **70**, 1019; (b) E.-I. Rõõm, A. Kütt, I. Kaljurand, I. Koppel, I. Leito, I. A. Koppel, M. Mishima, K. Goto and Y. Miyahara, *Chem. Eur. J.*, 2007, **13**, 7631.

16 (a) I. Krossing and I. Raabe, *Angew. Chem. Int. Ed.*, 2004, **43**, 2066; (b) H.-P. Wu, C. Janiak, G. Rheinwald and H. Lang, *J. Chem. Soc., Dalton Trans.*, 1999, 183.

17 (a) S. I. Kirin, H.-B. Kraatz and N. Metzler-Nolte, *Chem. Soc. Rev.*, 2006, **35**, 348; (b) S. I. Kirin, D. Wissenbach and N. Metzler-Nolte, *New J. Chem.*, 2005, **29**, 1168.

18 (a) Z. Kokan, Z. Glasovac, M. Majerić Elenkov, M. Grdičak, I. Jerić and S. I. Kirin, *Organometallics*, 2014, **33**, 4005; (b) Z. Kokan, S. I. Kirin, *Eur. J. Org. Chem.*, 2013, 8154; (c) Z. Kokan and S. I. Kirin, *RSC Adv.*, 2012, **2**, 5729.

19 Z. Otwinowsky and W. Minor, *Methods Enzymol.*, 1997, **276**, 307.

20 Oxford Diffraction, CrysAlis PRO, Oxford Diffraction Ltd., Yarnton, England, 2009.

21 G. M. Sheldrick, *Acta. Cryst*., 2008, **A64**, 112.

22 A. Altomare, G. Cascarano, C. Giacovazzo and A. Guagliardi, *J. Appl. Crystallogr.*, 2993, **26**, 343.

23 DIAMOND, v3.2, Crystal Impact GbR, Bonn, Germany.

24 J. Wang, R. M. Wolf, J. W. Caldwell, P. A. Kollman and D. A. Case, *J. Comput. Chem.*, 2004, **25**, 1157.

25 A. Jakalian, B. L. Bush, D. B. Jack and C. I. Bayly, *J. Comput. Chem.*, 2000, **21**, 132.

26 D. A. Case, T. A. Darden, T. E. III Cheatham, C. L. Simmerling, J. Wang, R. E. Duke, R. Luo, R. C. Walker, W. Zhang, K. M. Merz, B. Roberts, S. Hayik, A. Roitberg, G. Seabra, J. Swails, A. W. Goetz, I. Kolossvary, K. F. Wong, F. Paesani, J. Vanicek, R. M. Wolf, J. Liu, X. Wu, W. R. Brozell, T. Steinbrecher, H. Gohlke, Q. Cai, X. Ye, J. Wang, M.-J. Hsieh, G. Cui, D. R. Roe, D. H. Mathews, M. G. Seetin, R. Salomon-Ferrer, C. Sagui, V. Babin, T. Luchko, S. Gusarov, A. Kovalenko and P. A. Kollman, AMBER 12, University of California, San Francisco, 2012.

27 (a) E. A. Amin and D. G. Truhlar, *J. Chem. Theory Comput.*, 2008, **4**, 75; (b) C. J. Cramer and D. G. Truhlar, *Phys. Chem. Chem. Phys.*, 2009, **11**, 10757.

28 (a) Y. Zhao and D. G. Truhlar, *J. Chem. Theory Comput.*, 2011, **7**, 669; (c) Y. Zhao and D. G. Truhlar, *Acc. Chem. Res.*, 2008, **41**, 157.

29 M. J. Frisch, G. W. Trucks, H. B. Schlegel, G. E. Scuseria, M. A. Robb, J. R. Cheeseman, G. Scalmani, V. Barone, B. Mennucci, G. A. Petersson, H. Nakatsuji, M. Caricato, X. Li, H. P. Hratchian, A. F. Izmaylov, J. Bloino, G. Zheng, J. L. Sonnenberg, M. Hada, M. Ehara, K. Toyota, R. Fukuda, J. Hasegawa, M. Ishida, T. Nakajima, Y. Honda, O. Kitao, H. Nakai, T. Vreven, J. A. Montgomery Jr., J. E. Peralta, F. Ogliaro, M. Bearpark, J. J. Heyd, E. Brothers, K. N. Kudin, V. N. Staroverov, R. Kobayashi, J. Normand, K. Raghavachari, A. Rendell, J. C. Burant, S. S. Iyengar, J. Tomasi, M. Cossi, N. Rega, J. M. Millam, M. Klene, J. E. Knox, J. B. Cross, V. Bakken, C. Adamo, J. Jaramillo, R. Gomperts, R. E. Stratmann, O. Yazyev, A. J. Austin, R. Cammi, C. Pomelli, J. W. Ochterski, R. L. Martin, K. Morokuma, V. G. Zakrzewski, G. A. Voth, P. Salvador, J. J. Dannenberg, S. Dapprich, A. D. Daniels, Ö. Farkas, J. B. Foresman, J. V. Ortiz, J. Cioslowski and D. J. Fox, Gaussian 09, Revision A.02. Gaussian Inc.; Wallingford, CT, 2009.

30 The program Mercury is available at no cost from www.ccdc.cam.ac.uk/products/mercury.

Graphical abstract

for

Synthesis and characterization of ML and ML_2 metal complexes with amino acid substituted bis(2-picolyl)amine ligands.

Đani Škalamera,[a] Ernest Sanders,[a] Robert Vianello,[a] Aleksandra Maršavelski,[a] Andrej Pevec,[b] Iztok Turel[b] and Srećko I. Kirin*,[a]

[a] Ruđer Bošković Institute, Bijenička cesta 54, 10 000 Zagreb, Croatia.
E-mail: Srecko.Kirin@irb.hr
[b] Faculty of Chemistry and Chemical Technology, University of Ljubljana, Vecna pot 113, 1000 Ljubljana, Slovenia.

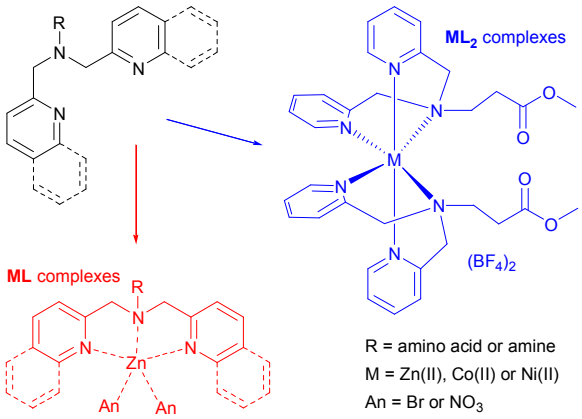

The stoichiometry and stereochemistry of bis(2-picolyl)amine (bpa) or bis(2-quinolidylmethyl)amine (bqa) metal complexes were studied by spectroscopy, crystallography and DFT calculations.